British Geological Survey

Developing a new ground electric field model for the UK based on long-period magnetotelluric data for the SWIMMR N4 (SAGE) framework

Multihazard and Resilience Programme

Open Report OR/24/022

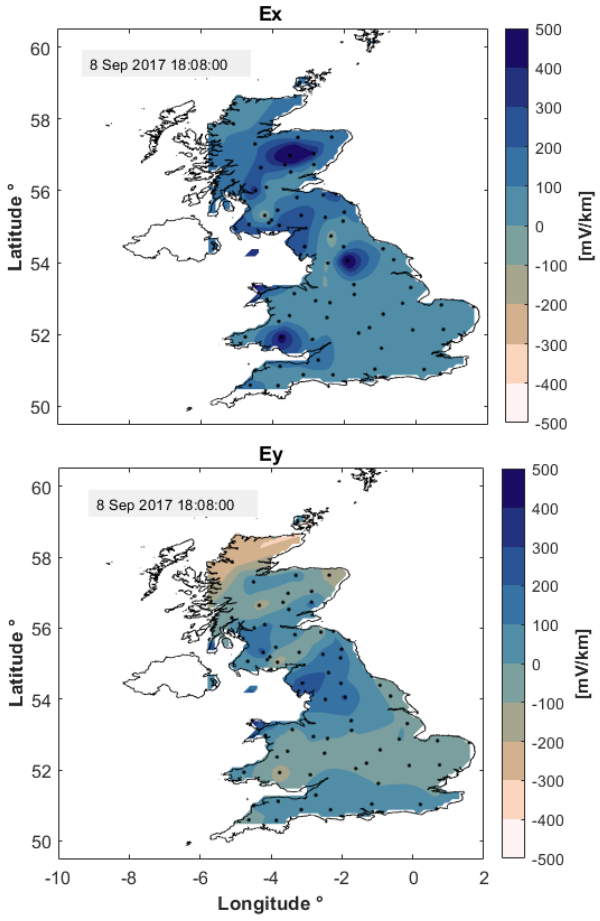

BRITISH GEOLOGICAL SURVEY

MULTIHAZARD AND RESILIENCE PROGRAMME

COMMISSIONED REPORT OR/24/022

Developing a new ground electric field model for the UK based on long-period magnetotelluric data for the SWIMMR N4 (SAGE) framework

J. Huebert, E. Eaton and C.D. Beggan

Keywords

Geoelectric field modelling; magnetotelluric measurements; space weather hazard; SWIMMR.

Front cover

Location of magnetotelluric measurements in Britain and the modelled maximum geoelectric field for 8 September 2017, 18:08

Bibliographical reference

Developing a new ground electric field model for the UK based on long-period magnetotelluric data for the SWIMMR N4 (SAGE) framework. *British Geological Survey Commissioned Report*, OR/24/022. 42pp.

Edinburgh British Geological Survey 2024

BRITISH GEOLOGICAL SURVEY

The full range of our publications is available from BGS shops at Nottingham, Edinburgh, London and Cardiff (Welsh publications only) see contact details below or shop online at www.geologyshop.com

The London Information Office also maintains a reference collection of BGS publications, including maps, for consultation.

We publish an annual catalogue of our maps and other publications; this catalogue is available online or from any of the BGS shops.

The British Geological Survey carries out the geological survey of Great Britain and Northern Ireland (the latter as an agency service for the government of Northern Ireland), and of the surrounding continental shelf, as well as basic research projects. It also undertakes programmes of technical aid in geology in developing countries.

The British Geological Survey is a component body of UK Research and Innovation.

British Geological Survey offices

Nicker Hill, Keyworth,
Nottingham NG12 5GG
Tel 0115 936 3100

BGS Central Enquiries Desk
Tel 0115 936 3143
email enquiries@bgs.ac.uk

BGS Sales
Tel 0115 936 3241
email sales@bgs.ac.uk

The Lyell Centre, Research Avenue South,
Edinburgh EH14 4AP
Tel 0131 667 1000
email scotsales@bgs.ac.uk

Natural History Museum, Cromwell Road,
London SW7 5BD
Tel 020 7589 4090
Tel 020 7942 5344/45
email bgslondon@bgs.ac.uk

Cardiff University, Main Building, Park Place,
Cardiff CF10 3AT
Tel 029 2167 4280

Maclean Building, Crowmarsh Gifford,
Wallingford OX10 8BB
Tel 01491 838800

Geological Survey of Northern Ireland, Department of Enterprise, Trade & Investment, Dundonald House, Upper Newtownards Road, Ballymiscaw,
Belfast, BT4 3SB
Tel 01232 666595
www.bgs.ac.uk/gsni/

Natural Environment Research Council, Polaris House,
North Star Avenue, Swindon SN2 1EU
Tel 01793 411500 Fax 01793 411501
www.nerc.ac.uk

UK Research and Innovation, Polaris House,
Swindon SN2 1FL
Tel 01793 444000
www.ukri.org

Website www.bgs.ac.uk
Shop online at www.geologyshop.com

Foreword

This document is the final report from the British Geological Survey (BGS) for the joint NERC-STFC Space Weather Instrumentation, Measurement, Modelling and Risk (SWIMMR) – Activities in Ground Effects (SAGE) programme on the production of a new *ground electric field* model for the UK. The report details the instrumentation, deployment, and measurement of the magnetotelluric campaign to collect new magnetic and geoelectric data at sites across the UK. These measurements are then used for a full UK-wide representation of the geoelectric field during space weather events. Finally, using the new data we re-visit GIC modelling for the UK power grid for two historic geomagnetic storms and outline the now- and forecast capabilities of Space Weather impacts on ground-based systems using the new geoelectric field model.

Acknowledgements

In addition to the authors, other BGS staff have contributed to the production of this report. Former Geomagnetism staff member Eliot Eaton contributed greatly to the collection of the new long-period magnetotelluric data. We thank him for his dedication and perseverance when dealing with landowners, equipment and field crew.

Aideliz Montiel Alvarez (University of Edinburgh) is thanked for her assistance and contribution to the field campaign. Nine LMT sites in Scotland were collected by her and with the help of funding from the Scottish Alliance for Geoscience, Environment and Society (SAGES) and a grant from the Royal Geological Society.

We further thank for assistance of the field work: Adam Collins, Helen Smith, Guanren Wang, Sarah Watson, Dave Morgan and Eleanor Maume. Lauren Orr has performed the extreme values analysis.

We thank our project partners, Colin Hogg and Duygu Kiyan, at the Dublin Institute of Advanced Studies (DIAS), Ireland for the loan of their long-period magnetotelluric instruments and support in maintaining them over the three year period of the project.

Finally, we thank the many landowners for allowing the use of their land for the temporary deployment of the magnetotelluric systems.

This project was funded under the NERC SWIMMR Activities in Ground Effects (SAGE), grant number NE/V002694/1 from June 2020 to March 2024.

Magnetotelluric measurements collected during this award are available on the NERC Geoscience Data Repository (NGDC[1]).

[1] https://www.bgs.ac.uk/geological-data/national-geoscience-data-centre/

Contents

FIGURES

TABLES

Summary

The large variations in ground electric field across the country during a geomagnetic storm drive so-called geomagnetically induced current (GICs), a major geohazard to ground-based technological infrastructure such as electrical transformers at high voltage substations, gas pipelines and railway signalling.

This report describes the collection of data and modelling work required to create a new ground electric field model for the UK developed by the SWIMMR N4 (SAGE) project. The model is based on new long-period magnetotelluric (MT) data collected across Britain during the SAGE project along with legacy MT data from previous surveys. MT data sense the electrical conductivity of the rocks in the subsurface down to large depths and allow images of the subsurface structure to be inverted for using sophisticated computational methods.

In this report, we describe the methodology, the fieldwork campaign to collect the MT data at 44 sites in Britain during a two-year field campaign from April 2021 to August 2023 and initial results of geoelectric field modelling. At each site, timeseries of electric and magnetic field variations were recorded continuously and simultaneously for several weeks. The raw data were then processed into MT impedance tensors at each site. The MT impedance data are then used to model geoelectric fields during geomagnetic storm times, showing large variations across the country due to the varying geology. A brief overview of the legacy MT data available from previous space weather-related projects and two historic MT campaigns are described.

We examine the modelled geoelectric field during the September 2017 and March 1989 geomagnetic storms using magnetic field measurements and the MT impedance tensor estimates. For example, in central Yorkshire the electric field estimates are about one-tenth of the magnitude observed in Lincolnshire around 100 km distant to the south, illustrating the spatial variability of the geoelectric field due to the underlying geology.

An outline for the implementation of ground electric field modelling for the now- and forecast framework in the SWIMMR N4 (SAGE) cloud-based modelling service is then presented. Our approach uses the MT impedances and magnetic field data measured at geomagnetic observatories across the UK. Some measures to account for the limitations of frequency-domain modelling are applied. In the future, the geoelectric field modelling can be based on a full 3D inversion model of UK subsurface electrical conductivity using the MT data collected.

We also briefly outline how the new model in combination with the decades-long magnetic field observations in the UK will be used to assess space weather hazards in the context of extreme value analysis and hazard maps.

1 Introduction

During severe space weather events, the Earth's magnetic field can change rapidly with large variations in the order of thousands of nT at mid-latitudes (Rogers *et al.,* 2020; Thomson *et al*., 2011). The time variations of the externally driven magnetic field induce geoelectric fields in the conductive ground, whose magnitude and spatial scale depend on the underlying electrical conductivity structure. For long period variations (tens to hundreds of seconds) in resistive geology, the skin depth is large (100-1000 km) and the magnetic field generates a relatively large geoelectric field. Short period variations (less than 10 seconds) of the magnetic field in a conductive subsurface have shallow skin depths (0.1-1 km) and produce relatively weak geoelectric fields (e.g., Campanya 2017).

Strong geoelectric fields, which can be up to several tens of V/km in some locations (Love *et al.,* 2018), build up over large areas posing a hazard to certain types of modern technology. With widespread adoption of low-resistance grounded infrastructure, such as high voltage (HV) power networks, induced geoelectric fields can more readily equalise through the earthing points of these conductors. These quasi-steady DC currents are called Geomagnetically Induced Currents (GICs), though small in comparison to the load carried, are a threat to the safe and optimal operation of HV transformers (Boteler, 2006; Pulkkinen *et al*., 2012). A well-known example of damage from GICs is the failure of the Québec-Hydro network in March 1989 (Bolduc, 2002; Boteler, 2019). The present-day cost of a similar widespread and long-lasting power outage could be of the order of tens of billions of US dollars per day (Oughton *et al.*, 2018).

Geomagnetically induced currents are therefore recognised as a potential hazard to electrical power transmission systems across the world, particularly at higher latitudes or in regions with lengthy high-voltage transmission lines. The first step in understanding this hazard is to quantify the induced geoelectric (or telluric) field at the Earth's surface. Unfortunately, long-term measurements of the geoelectric field are rare and are only available at a few locations around the world including Hungary, Japan, the USA and the UK.

Most hazard assessment relies on geoelectric field modelling based on measurements from magnetotelluric surveys and detailed computationally intensive 3D conductivity modelling (e.g., Rosenqvist *et al.,* 2022). Magnetotellurics is a widely used EM deep-sounding method to image the subsurface electrical conductivity (or its inverse, the electrical resistivity) in varying scales, from shallow subsurface to crustal targets and global induction studies. MT has been used intensively in mineral exploration, geothermal and environmental surveys and to investigate tectonic and volcanic settings but such datasets are often commercially valuable and hard to access. The depth of investigation depends on the period or frequency of the recorded signal variations in the magnetic and electric field at the surface of the Earth. Longer period/lower frequency signals penetrate deeper into the crust, whereas higher frequencies/short periods probe the shallower subsurface. Long-period MT (LMT) employs fluxgate magnetometers to capture the magnetic field variations and is mostly utilized to study the structure of the lower crust and mantle. Higher frequency data are collected with broadband equipment including induction coil magnetometers.

More recently it was realized that MT data over larger regional scales can be used to help characterize space weather impact on ground infrastructure through modelling of the ground electric field during geomagnetic active times, and that there is therefore a need to collect new and reuse older and legacy data (Ayala *et al.*, 2022). There are efforts to encourage sharing of MT data in a similar way to that of seismic and geomagnetic data, but these have been slow to produce outputs due to the generally more restrictive conditions on reuse of MT data.

In the absence of large MT datasets, many initial attempts to characterise the ground electrical conductivity have involved synthetic models based on geologic data and considerations. In the UK, a thin-sheet conductance model of the upper 3 km has been developed over the past two decades (Beamish, 2013; McKay, 2003). It is based on airborne electromagnetic (EM) data and laboratory measurements of electrical conductivity. With these models, regional electrical fields can be computed using the thin-sheet approach first conceived by Vasseur and Weidelt (1977), albeit with relatively large uncertainties (Beggan, 2015).

Until recently, BGS capability in geoelectric field modelling have included the thin-sheet conductivity model and an underlying 1D model of electrical conductivity of the lithosphere to produce time varying estimates of the geoelectric field at a 10 km resolution across the UK. This method has the advantage of being computationally fast, but it is known to generally underestimate the magnitude of the geoelectric field when compared to measured values (Beggan *et al.* 2021) and we show in this report that in many locations in the UK it is not particularly accurate.

As part of the NERC-STFC funded Space Weather Instrumentation, Measurement, Modelling and Risk (SWIMMR) programme, one major objective in the N4 SWIMMR Activities in Ground Effects (SAGE) project was to substantially improve existing geoelectric field modelling capability in the UK. We achieved this by: (i) making new magnetotelluric measurements for space weather purposes in England and Wales to supplement existing MT data; (ii) producing a new and more accurate ground electric field model of the UK and Ireland; and (iii) implementing the new modelling capability for real-time now-cast and forecast of the geoelectric field to allow the computation of GICs in the UK high voltage power system, high pressure pipeline network and rail systems.

The project was scheduled to begin in September 2020, but fieldwork to collect new MT data across England and Wales suffered from a six month delay due to travel restrictions during the Covid-19 pandemic in 2020/21. All new MT data collected will be used to construct a new full 3D model of electrical conductivity below the British Isles, utilizing sophisticated inversion algorithms and prior information about bathymetry and littoral sediments. An ongoing PhD project (as of mid-2024) in conjunction with University of Edinburgh will help to achieve this.

The report presented here outlines the initial work by BGS to meet the stated goals and presents methodology and results obtained so far (August 2022). In Section 2 we describe the existing data and models, their origin and suitability for space weather forecasting. Section 3 describes the magnetotelluric field campaign of 2021 to 2024 and a review of legacy MT data. In Section 4 we discuss and interpret results of improved geoelectric field modelling within the SAGE framework and outline the operational geoelectric field models for now- and forecasting of space weather impact on ground-based structures. We briefly discuss how a full 3-D inversion model derived from the new data will further improve geoelectric field modelling. Finally, we describe how the new data are used to further assess the risks of space weather on ground-based infrastructure by using Extreme Value Analysis (EVA).

2 Modelling the Ground Electric Field for Space Weather Impact Assessment

Time-varying electric and magnetic fields occur naturally in the ground and induce each other as expressed through Maxwell's equations. The ground electric or geoelectric field during geomagnetic storms is induced via the disturbed geomagnetic field and is also directly dependent on the ground electrical conductivity. During storm times, it laterally varies much more in comparison with the magnetic field because electrical charge carriers are very unevenly distributed in the subsurface. The ability to transport electric current in rocks is captured in the bulk electrical conductivity (or resistivity). Conductivity is a wide-ranging rock parameter and depends mostly on the composition, pore space and fluid content of the rocks. For example, a porous fluid-saturated sandstone is a much better conductor than a dense young granite. The best electrical conductors in the context of geology are metals, melts and graphite.

Ground electric fields are generally quite small (in the range of mV/km) and can be measured via the potential difference between two metallic electrodes. For longer term measurements, non-polarizable electrodes are needed to avoid the build-up of charges due to electrochemical reactions.

To characterize the electric field over an area as large as the British Isles in real-time, we need a large number (>50) of instruments measuring the geoelectric field. However, permanent deployment of such equipment is expensive and needs a large resource to quality-check and maintain. In the UK, the ground electric field is currently monitored at three sites (the GB geomagnetic observatories in Lerwick, Eskdalemuir and Hartland) and the data collected there were described in Beggan et al. (2021). The sparse direct observations of the electric field make it necessary to develop numerical models to cover the gaps between measurement locations and allow for modelling of Space Weather impacts such as GICs.

There are several approaches for calculating the geoelectric field during geomagnetically active times (Kelbert, 2020). For modelling in the UK, three main approaches have been discussed (Beggan et al., 2021): (i) 2D maps of the electric field at the surface created from a thin-sheet conductance model of the British Isles; (ii) models of the ground electric field derived using the MT impedance tensor at specific sites; (iii) full 3D estimates of the electric field based on a 3D inversion model of electrical conductivity derived from MT measurements.

All models of the ground electric field were compared to direct measurements at our observatory sites, and we found that using the magnetotelluric impedance tensor produced more realistic geoelectric fields.

2.1 THE MAGNETOTELLURIC METHOD

The magnetotelluric (MT) method is a deep-sounding geophysical technique that uses the principles of electromagnetic induction to study the interior of the earth. By simultaneously recording the variations in the natural magnetic and electric field on the surface of the earth it is possible to derive models of underlying electrical conductivity. In practice, a magnetic sensor (for long period recordings, a three-axial fluxgate magnetometer is used) samples the magnetic field in cartesian coordinates (x-north, y-east, z-downwards) every second. The horizontal electric field is measured with two dipoles. The recorded time series are filtered and transformed into frequency spectra which can then be used to derive the impedance tensor **Z**.

The impedance tensor is defined in the frequency domain ($\omega=2\pi/f$) and relates the variation of the magnetic field (**B**) to that of the electric field (**E**):

$$\mathbf{E}(\omega) = \frac{1}{\mu_0}\mathbf{Z}(\omega) \cdot \boldsymbol{B}(\omega)$$

where μ_0 is the permeability of free space. The **Z** tensor has four complex components:

$$\mathbf{Z} = \begin{pmatrix} Zxx & Zxy \\ Zyx & Zyy \end{pmatrix}$$

and is often displayed as apparent resistivity (a measure for the amplitude and the true resistivity if the subsurface is homogeneous) and phase curves for each component. These are defined as:

$$\rho_a = \frac{1}{\omega\mu_0}\left|Z_{ij}\right| \text{ and } \Phi = \tan^{-1}\left(\frac{Im(Z_{ij})}{Re(Z_{ij})}\right)$$

$$ij = x, y$$

Apparent resistivity and phase allow for a quick visual inspection of quality of the data at each site as well as the magnitude and changes in conductivity in the subsurface with depth.

For spatial visual inspection of MT survey data from multiple sites, phase tensors are often derived and plotted (Caldwell *et al.*, 2004). Phase tensors have the advantage that they are not influenced by local galvanic distortion. For the MT impedance $Z = X + iY$ they are defined as:

$$\Phi = X^{-1} \cdot Y$$

The phase tensor can also be characterised by its three invariants, Φ_{min}, Φ_{max} and β (see Figure 1).

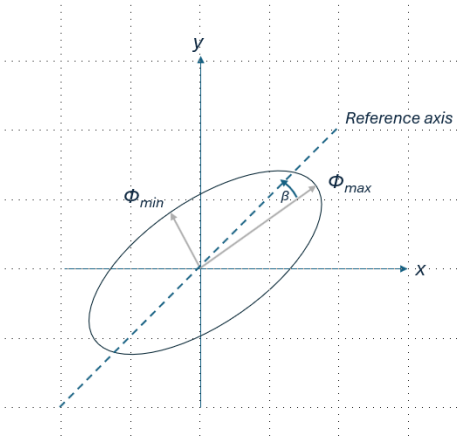

Figure 1: The three invariants of the magnetotelluric phase tensor.

In the absence of active geologic processes that could change the composition or electrical conductivity of the underlying rocks over time, the impedance tensor is assumed to be temporarily independent.

The inducing magnetic field is assumed to be spatially uniform, and **Z** is considered quasi-stationary (independent of when the recordings were performed) and only dependent on the local Earth response (i.e. geology). Typically, MT recordings last from a few days to a couple of months. The length and quality of the data determines the frequency range of the computed transfer function, with the depth of investigation controlled by the skin depth of the EM waves.

Assuming a plane wave magnetic field impulse is driving the induced geoelectric field, the derived impedance tensor can be used to estimate the induced geoelectric field in a wide frequency range at any other time when only magnetic field data are available (Campanya *et al.*, 2019; Hübert *et al.*, 2020; Lucas *et al.*, 2018). Thus, the MT impedance tensor only needs to be correctly measured *once* and can be used to compute an estimate of any future geoelectric field if a magnetic field time-series at the location is available.

3 New Long-period Magnetotelluric Data

3.1 SAGE MT FIELD CAMPAIGN – SITE SELECTION

Within the SWIMMR N4 SAGE project, BGS Geomagnetism was tasked with the collection of new MT data across England and Wales to complement existing data and to make measurements Great Britain with approximately evenly distributed 50-70 km distance between sites, omitting large urban centres. Since MT is a passive method where signal-to-noise ratios are site-dependent, the careful selection of site locations is a priority. Ideally, the site is well away from all man-made electromagnetic signal sources like railway lines (>10 km), electric fences and power lines (>1 km), industry (>5 km), housing and generators (>2 km); this is similar to the recommendation for magnetic observations (Jankowski & Sucksdorff, 1997). Data collection for long-period signals takes at least four weeks, so the site should be mostly undisturbed by people and livestock. All sensors are buried to about half a metre depth and well away from tree roots. Open skies for GPS signal and solar panel recharge are also necessary. As far as possible, we pre-selected sites using satellite images and open-source information on the location of railway and power lines. For example, Figure 2 illustrates the distances between MT sites, HV power lines and railways in Cornwall. We thank all landowners and especially the National Trust for facilitating use of their land.

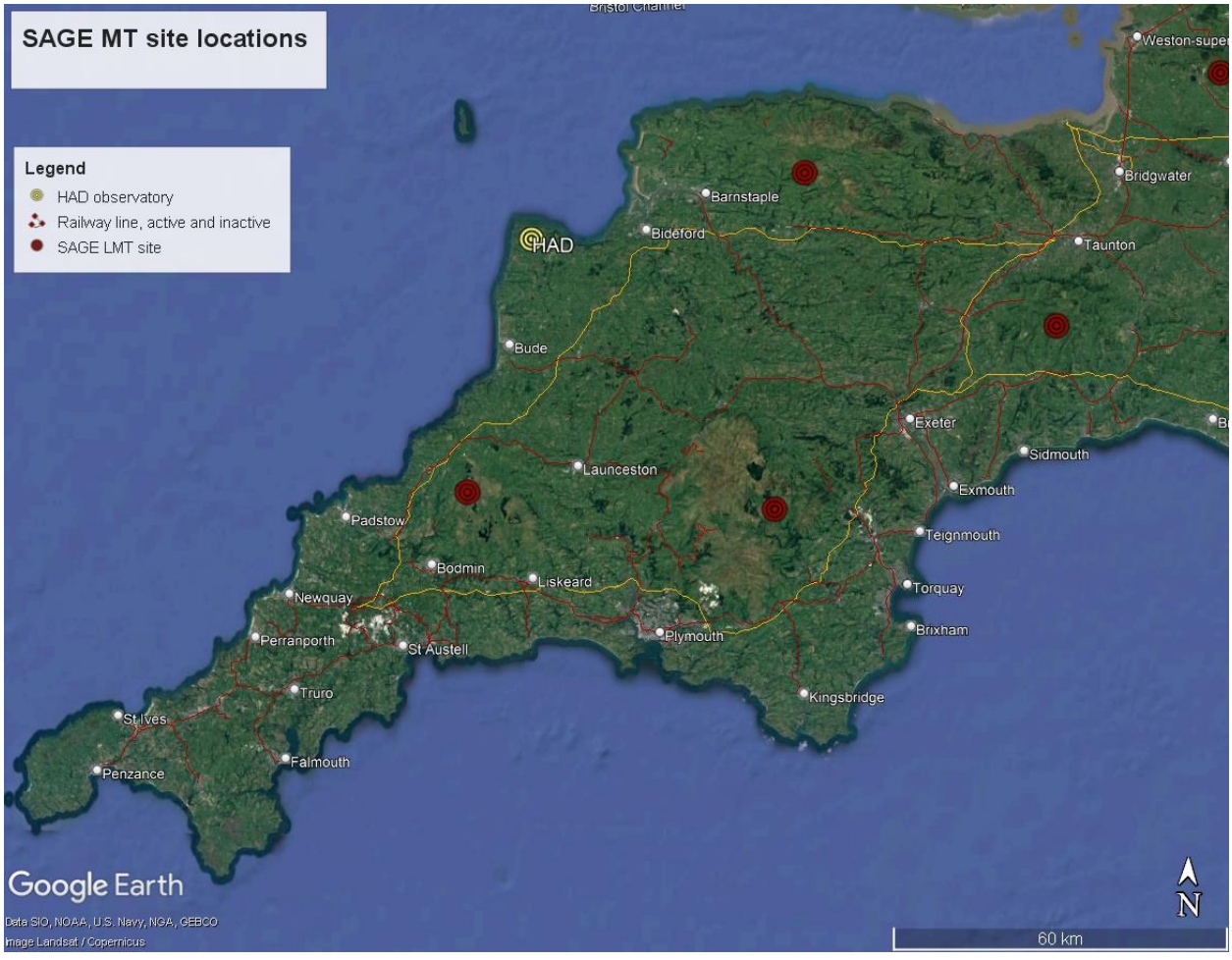

Figure 2: Location of HV transmission lines (orange lines) and (active and in-active) railway lines (red lines) and are shown together with the chosen locations for LMT sites (red circles) and Hartland observatory (HAD). Contains data from Google Earth with embedded attributions from Data SIO, NOAA U.S. Navy, NGA, GEBCO, Image Landsat / Copernicus; transmission network data © National Grid UK and data from OpenStreetMap.

3.2 INSTRUMENTATION AND INSTALLATION

For the field campaign, our project partners at the Dublin Institute for Advanced Studies (DIAS) provided four Lemi–417 magnetotelluric instruments including electrodes from their MT instrument pool (Figure 3). Electric field cables, solar panels including regulators and deep-cycle batteries as well as enclosures were purchased by the SAGE project and assembled in-house in the BGS office in Edinburgh.

The typical layout of an MT site can be seen in Figure 4Figure 4. A site installation in Northumberland can be seen in Figure 5. Special care is taken to ensure that the electric probes have good ground connection by watering them well once buried. We checked the contact resistances between dipole pairs and if this was higher than >10 kΩm, electrodes were replaced. Higher contact resistances generally signify degradation of the probes and this can lead to higher noise levels and jumps in the self-potential. The fluxgate magnetometer is aligned to magnetic East by manual rotation, minimizing the By component (and maximising the Bx value). Lemi magnetometers are watertight and robust with regard to temperature variation but burial helps reduce strong diurnal changes.

All cables are buried in shallow trenches to avoid damage from weather or livestock. The MT timeseries data are recorded in the Lemi-specific binary format in five separate channels (Ex, Ey, Bx, By and Bz). Information from temperature and battery life are recorded as well. Once the recording has finished, the data are downloaded and converted into ASCII format to subsequently process into impedance tensors. We inspected data quality at each site on the day after the installation to make sure that everything was recording correctly.

Due to the travel restrictions in relation to the Covid-19 pandemic, the start of the field campaign was delayed from October 2020 to April 2021. However, a no-cost extension of six months by both NERC and DIAS for the instrument loan until September 2023 allowed us to complete the field campaign. Further data were collected from October 2023 to March 2024 by Aideliz Montiel-Avarez to supplement the coverage in Scotland for her PhD research programme.

MT data collection followed a roll-on approach with continuous deployment of the four systems in use. We installed on average two to three sites each month. Some initial instrumental problems in Spring 2021 required the replacement of two Lemi units. The instruments were transported back to Ireland and then to the manufacturer in Ukraine for a software update before coming back to BGS. An additional software update was performed in August 2022 by BGS personnel.

Figure 3: Looking down on a Lemi-417 fluxgate magnetometer in the field, placed on a concrete slab for stability.

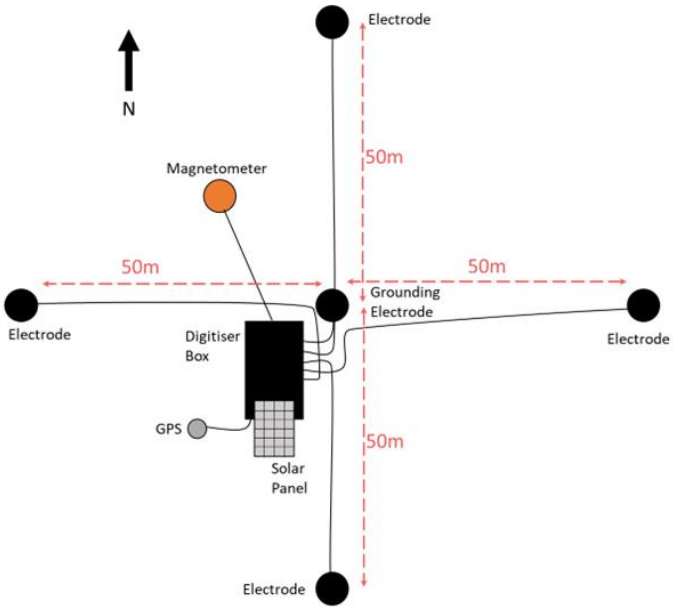

Figure 4: Plan view of layout of LMT site with sensor and recording components noted.

Figure 5: MT installation NY69 in Kielder Forest, Northumbria. All cables are buried to avoid interference from livestock. A small solar panel is constantly recharging the batteries. Visible is also the GPS antenna (white mushroom on a pole).

3.3 DATA COLLECTION: APRIL 2021 – AUGUST 2023

In total 44 new LMT sites have been installed within the SAGE project. We chose a naming convention based on Ordnance Survey grid references, with two letters and two numbers. This allows us to incorporate older sites and legacy measurements with a location-keyed naming convention. The locations of MT sites collected during SAGE can be seen in Figure 6 together with a bedrock geology map of the UK.

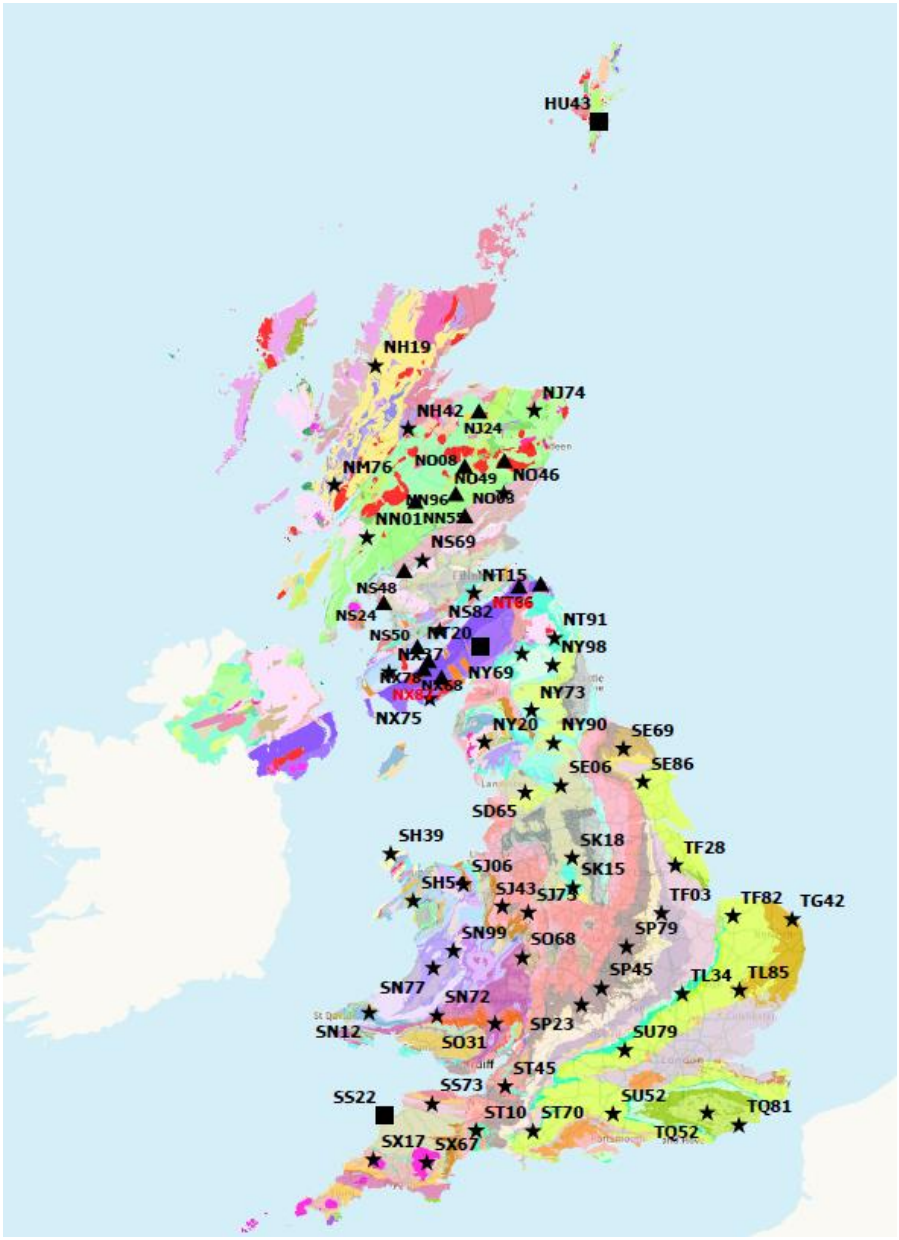

Figure 6: Location of SAGE MT sites and bedrock geology of the UK. Squares – UK geomagnetic observatories, stars – LMT sites within SWIMMR-SAGE, triangles – legacy LMT sites. For the geologic units we refer the reader to the BGS geology viewer[2]. Contains OS data © Crown Copyright and database right 2020.

[2] https://www.bgs.ac.uk/map-viewers/bgs-geology-viewer/

Visual inspection of the collected data allows an initial evaluation of data quality. For a high-quality recording, the magnetic and electric fields change smoothly and simultaneously. Rapid changes due to influences from space weather should be correlated between magnetic and electric channels. Figure 7 shows an example from site SX17 in Cornwall. The data show very good quality with the natural daily variations in the fields clearly visible as well as several periods of increased geomagnetic activity. Figure 8 shows the power spectra for each of the five MT channels computed via a Fourier transform from the timeseries data visible in Figure 7. No significant noise sources were recorded at this side.

Most SAGE sites have good data quality, but some suffered from disturbed electric field recordings. This might have been caused by local noise, but also by degradation of the probes. Some sites have very good electric field data, showing clearly the daily variations and smaller scale changes due to solar influence.

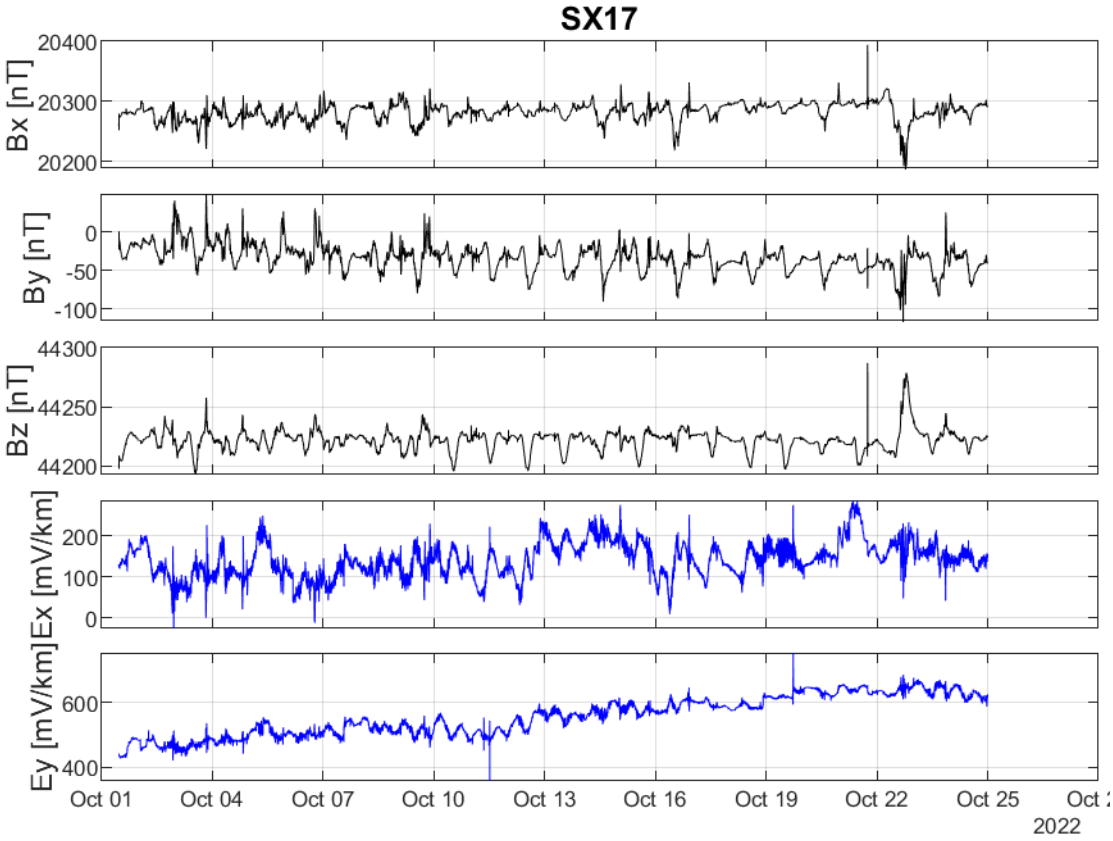

Figure 7: Example of three weeks of timeseries recorded at SX17 (Cornwall). Each panel shows one component of the five MT channels (three magnetic and two electric). Daily variations are clearly visible as well as some long-term drift in the electric fields. Several minor geomagnetic storm times were captured on 3, 15, 22 and 23 October 2022.

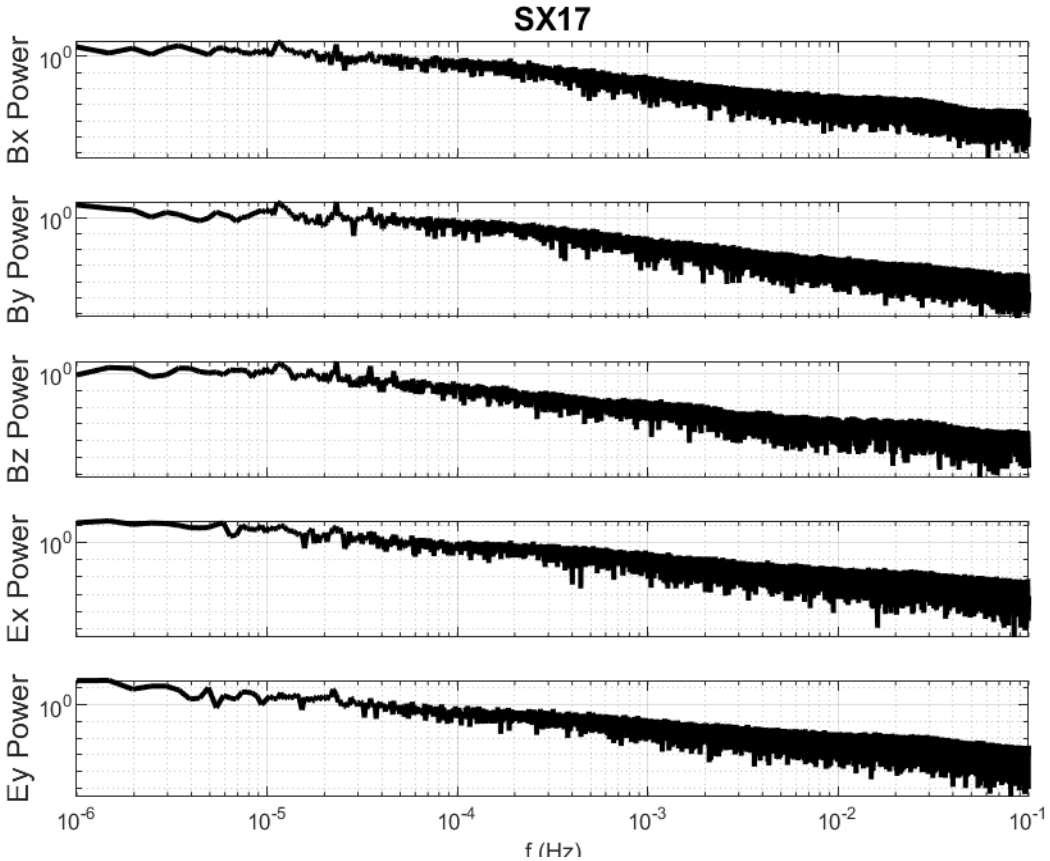

Figure 8: Power spectra computed from three weeks' time series measured at SX17.

3.4 ADDITIONAL NON-SAGE MT MEASUREMENTS

An additional nine sites were collected during October 2023 and March 2024 by A. Montiel Alvarez from University of Edinburgh with support from BGS to improve spatial coverage of Scotland. These data were recorded during the Scottish winter with challenging weather and wet ground conditions. For example, the installation in South Lanarkshire (NS82) had to be restarted after equipment failure in early January 2024. Nevertheless, data quality was deemed very good at all sites, and they were incorporated into the new BGS geoelectric field model.

Further LMT measurements are planned in the future to fill some gaps around infrastructure such as the railway lines. MT data from the Republic of Ireland and Northern Ireland measured by DIAS will be incorporated into future conductivity models of the entire British Isles.

3.5 TIME SERIES PROCESSING TO DERIVE MT IMPEDANCE TENSORS

In order to derive the impedance tensor from the timeseries, the processing code of Smirnov (2003), licenced to the BGS, was used. This software has a graphical user interface (GUI) that allows the fine tuning of the processing parameters that will regulate the impedance estimation. In the first step, the time series must be corrected for dipole length and system response. After the Fourier transform, a robust estimator finds the optimal impedance estimates and provides information on the uncertainty estimates. The GUI provides options to manipulate the data with several statistical tools and to generate output files in a variety of data formats. Remote referencing (see Gamble *et al.*, 1979) is a vital tool to improve data quality by reducing local noise. Remote referencing uses the magnetic field observations from either the geomagnetic observatories or simultaneously recording MT instruments at a different location to improve the quality of the impedances and decrease the uncertainties from local interference.

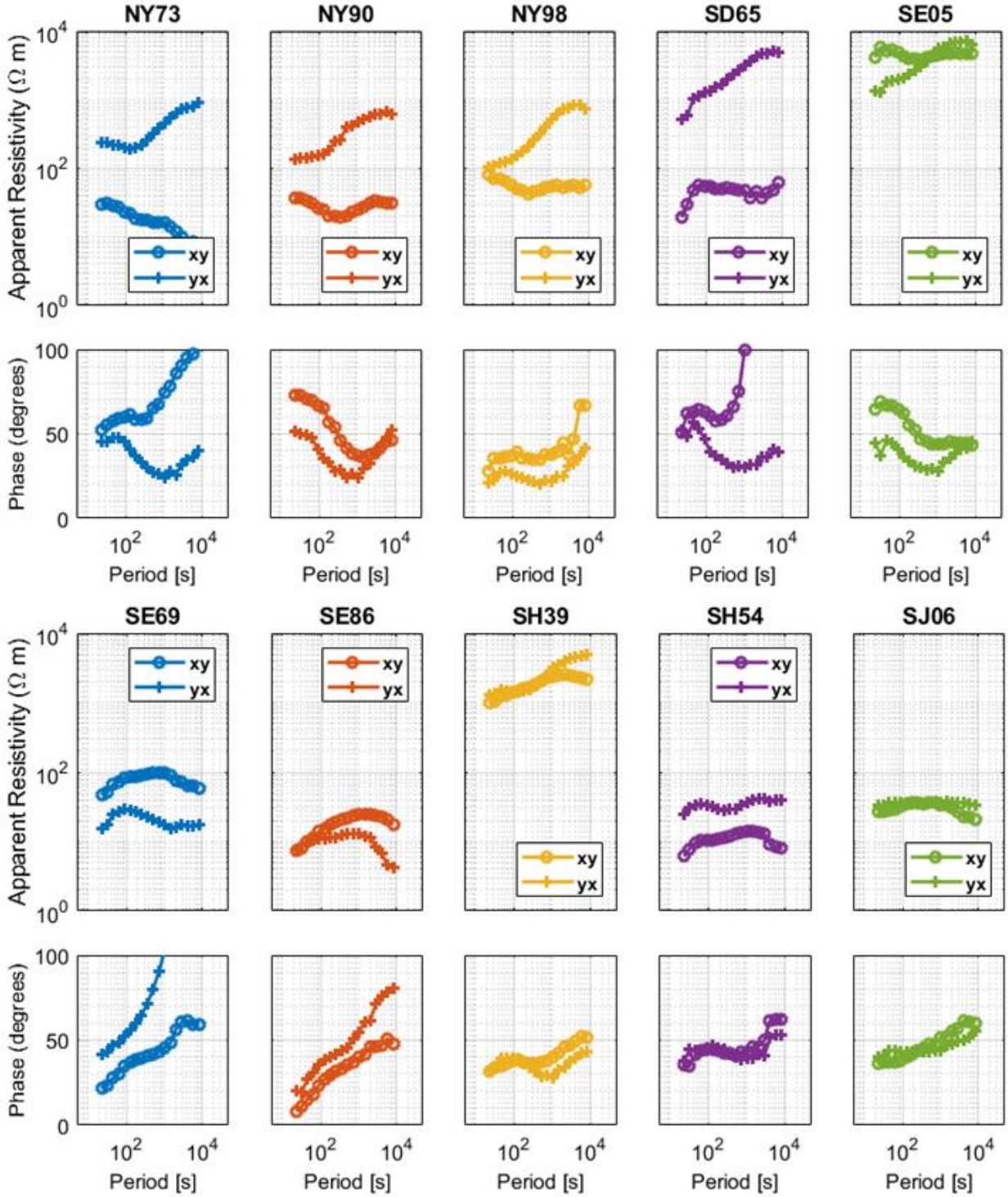

Figure 9: Apparent resistivity (upper) and phase (lower panels) of the main components Zxy and Zyx of the MT impedance tensor at 10 locations in the UK. The different magnitudes of apparent resistivity curves illustrate the varying amplitude of the local geoelectric field which is controlled by regional geology. The phase values indicate the complexity of the underlying conductivity distribution. All other impedances can be found in the appendix.

The frequency-dependent transfer functions for ten sites are presented in Figure 9 as apparent resistivity and phase of the off-diagonal impedance elements. The magnitude of the apparent resistivity gives an indication of the variation of electrical conductivity across Britain.

In a map view of all MT data displayed as magnetotelluric phase tensors for six different periods (longer periods indicate deeper levels of investigation), this also becomes evident (Figure 10). The phase tensors' shape and colour indicate the large variability of electrical conductivity at different depth levels in the UK.

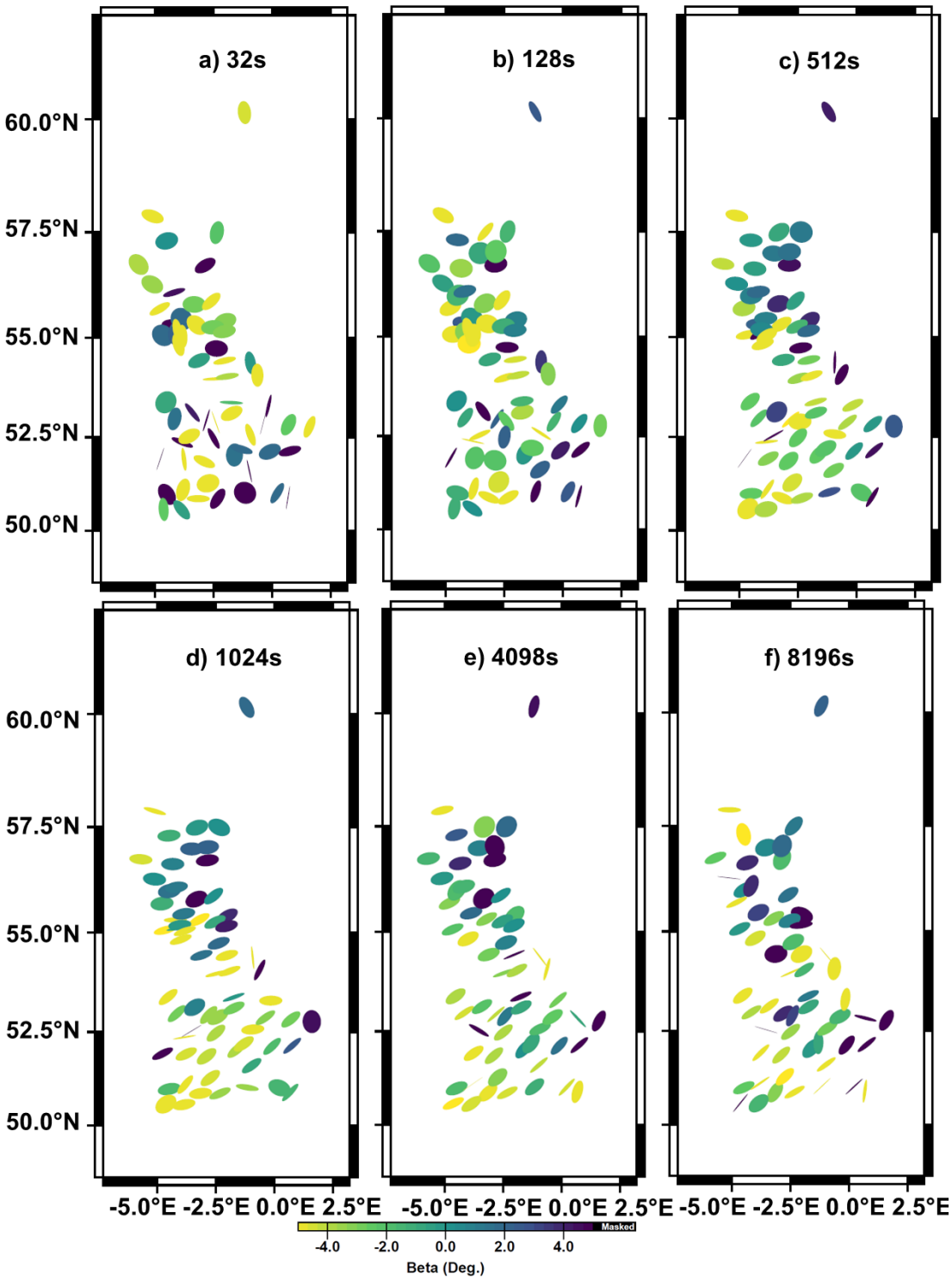

Figure 10: MT phase tensor estimates for SAGE MT sites and legacy data for six different periods: a) 32 s, b) 128 s, c) 512 s, d) 1024 s, e) 4098 s and f) 8196 s. In general, the more elliptically shaped a phase tensor, the more dimensionally complex the subsurface must be. The short periods represent more local geology with greater spatial variations, whereas the longer periods capture larger scale structures in the lower crust and upper mantle. The colours represent the skew angle β, another measure for the complexity of the subsurface.

In a final step to harmonize the impedance tensors from SAGE and legacy data before the geoelectric field modelling, we excluded periods longer than 20,000s (around 4 hours), smoothed the transfer functions with a factor of 1.5 and interpolated onto seven values per frequency decade using KMSPro. Figure 11 shows an example of the smoothed curve with seven points per order of magnitude in frequency.

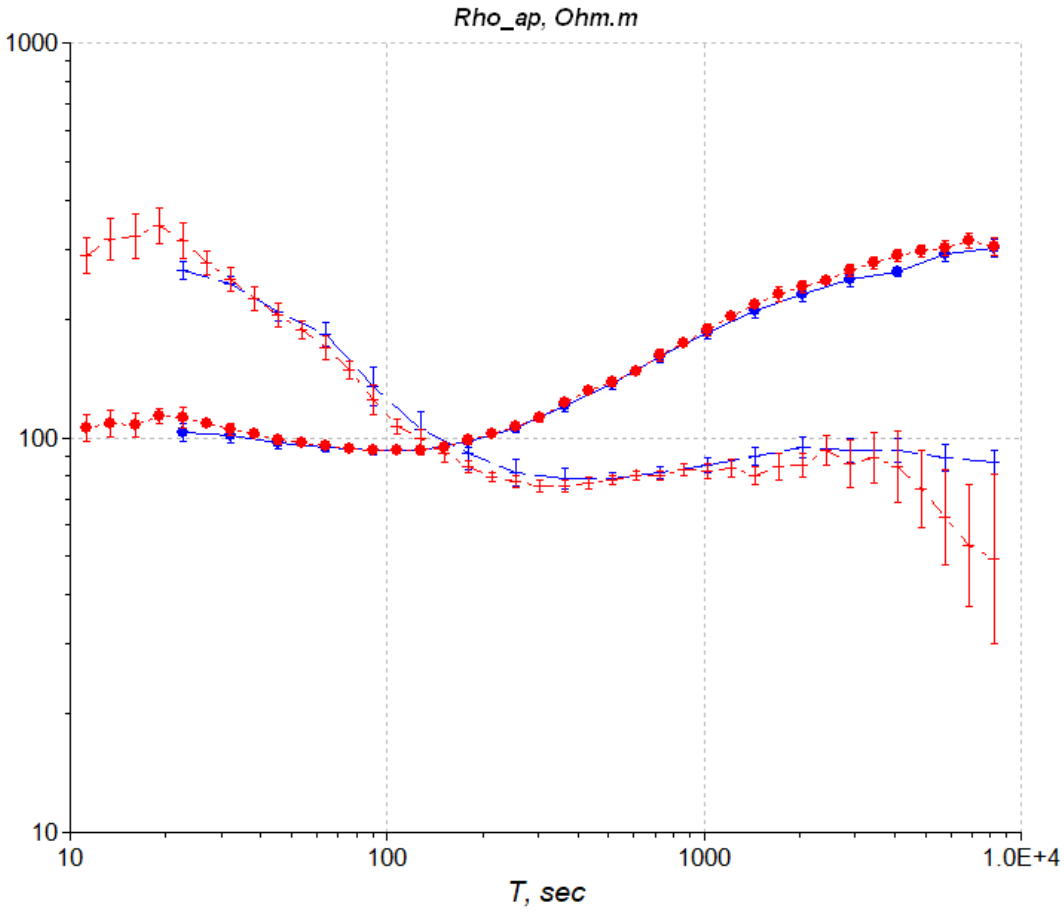

Figure 11: Apparent resistivity for site NT66 (Whiteadder, East Lothian). Red curves are the apparent resistivity values (circles for Zxy, crosses for Zyx component) derived from MT timeseries. Blue curves are the selected estimates from interpolation, smoothing and excluding values below 20s. These are used for the geoelectric field modelling.

3.6 LEGACY MAGNETOTELLURIC DATA IN BRITAIN

Magnetotelluric data in the UK have been collected for several decades. Unfortunately, not all of the data have been archived in data repositories. We have made every effort to obtain digital copies from authors and describe here the legacy data that were included.

- Simpson & Bahr (2020): Seven long-period MT stations were collected in Scotland as part of a larger data set collected within the SWIGS project. Available timeseries data are sampled at 32s which provides limited frequency bandwidth. Not all data from this survey were of sufficient data quality. Data retrieved from the NGDC.
- Huebert *et al.* (2020): Two long-period MT stations collected during SWIGS in east and west Scotland, with full frequency bandwidth available. This BGS-owned data is accessible at NGDC.
- Banks: a collection of legacy MT data in Scotland recorded before 1999. Made available by Roger Banks, cited as Junge *et al.* (1994). The original timeseries are not available,

only the processed impedance tensors with limited frequency bandwidth. As it is part of a larger data set, we selected the best quality sites from visual inspection.

- Tauber *et al.* (2003): From Dumfries and Galloway (Scotland) a broadband data with limited frequency bandwidth. Made available by R. Banks. Part of a larger data set, the original timeseries raw data are not available, only estimates of the impedance tensor. Four of the visually best sites were chosen with the widest geographical spread of locations

For the locations of all sites, see Table 1 in the Appendix.

3.7 DATA ACCESS

Magnetic and geoelectric field timeseries from the 44 MT sites collected by the SAGE are deposited in the NERC Geoscience Data Centre (NGDC) and be openly accessible. Search for 'Magnetotelluric' as a keyword.

The transfer functions will be incorporated into the geoelectric field modelling procedures for the SAGE cloud-based now- and forecast service for modelling space weather impacts on grounded infrastructure (the GIC and PSP model).

At the end of the PhD programme and, after a grace period for the PhD project to publish its findings, the 2023/24 Scottish MT datasets will be deposited in the NGDC.

4 Modelling geoelectric fields using MT impedances

With the new MT data set it is now possible to estimate the geoelectric field during geomagnetic storm times over the island of Britain both in real-time and in retrospect.

4.1 MODELLING GEOELECTRIC FIELDS FOR TWO STORMS

Using an adaptation of the algorithm presented in Campanya *et al.* (2019), we calculated the electric field at all sites using geomagnetic field measurements from three UK observatories and three international observatories for the March 1989 and from 15 stations for the September 2017 storms. The first step is to characterise the magnetic field variation across the island. This is done by using magnetic field measurement and an interpolation method called spherical elementary current systems (SECS) interpolation (MacLay and Beggan, 2010). The availability of magnetic field data varies for historical storms but is highest for the past decade (post-2014), when, in addition to the UK, neighbouring countries' geomagnetic observatories data with high quality and sampling rates were collected along with several variometer sites.

We present the geoelectric field model for two geomagnetic storms of the past decades: the March 1989 storm that caused wide-spread ground effects especially in Canada; and the September 2017 storm which is well documented in the literature.

For the Spherical elementary current system (SECS) interpolation for *September 2017*, minute-mean cadence data were available from the three UK observatories (ESK, LER, HAD[3]), other European observatories around the North Sea (CLF, DOU, VAL, WNG[4]) and variometer sites from the Lancaster SAMNET and BGS School Magnetometer Network (ARM, BGS09, BGS10, BIR, CRK, DOB, HOV, SOL, KAR, SID) were used (see Beggan and Marple, 2018 for locations). For the SECS interpolation for the *March 1989 storm*, 1-min magnetic field data from UK observatories (ESK, LER, HAD), other European observatories (CLF, VAL, WNG) are available.

The magnetic field timeseries for between two and three days were derived from the SECS model at each MT site location. The magnetic timeseries were Fourier transformed to compute the equivalent values in the frequency domain. The Fourier coefficients for the horizontal magnetic field components (Bx and By) are multiplied by the impedance values at each site and then inversely Fourier transformed into time series again. This produces a timeseries of the geoelectric field at each MT site during the storms.

We estimated the peak values of geoelectric fields, both Ex and Ey direction as well as an average of the horizontal electric field (|Eh|) at all sites. These are plotted in Figure 12 and Figure 13.

There are differences in the spatial distribution of the highest geoelectric field amplitudes. For the 2017 storm, there is a clear dependency of higher amplitudes with higher latitude, showing maximum values for the Scottish Highlands. However, for the 1989 storm, the highest geoelectric field values were reached in the Peak district and the Midlands of England. This is related to the strong equatorward expansion of the auroral oval during this major geomagnetic event.

[3] Using their IAGA abbreviations here: ESK- Eskdalemuir, LER – Lerwick, HAD- Hartland
[4] CLF- Chambon-la-Forêt, France; DOU- Dourbes, Belgium; VAL - Valencia, Ireland; WNG – Wingst, Germany.

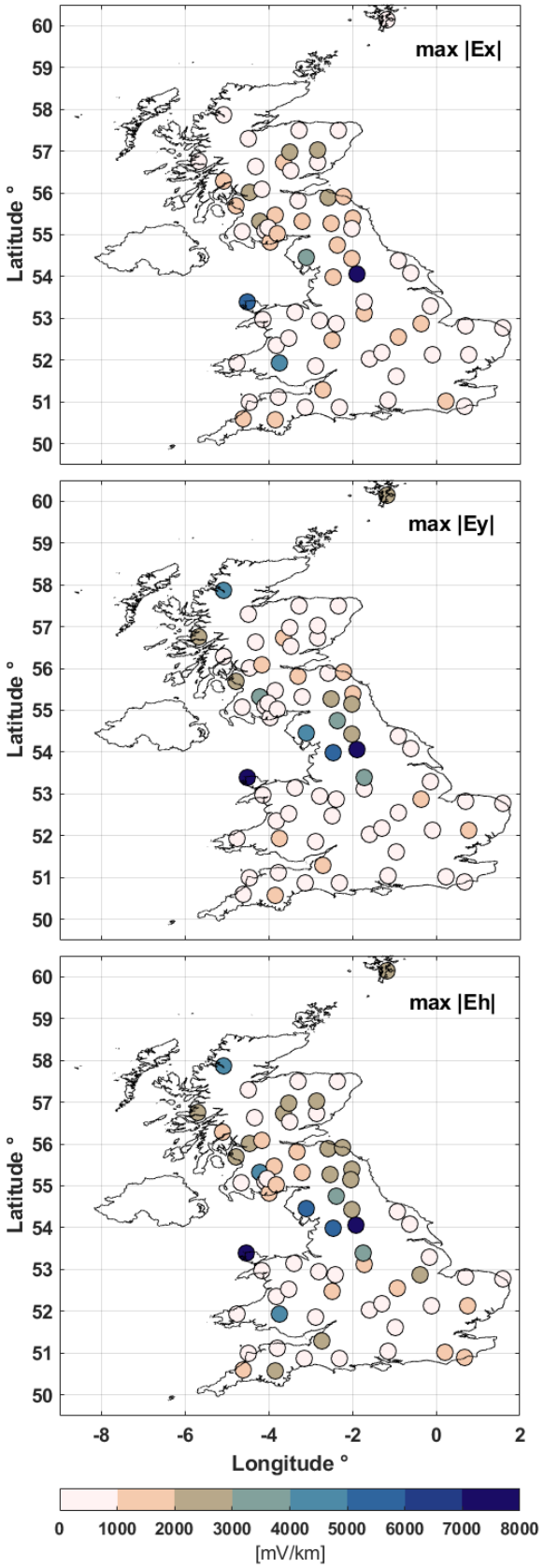

Figure 12: Maximum electric field values during the March 1989 storm in the north (Ex), east (Ey) and total horizontal field (Eh). Units of milliVolts per km. The highest values of >8,000 mV/km were modelled for Anglesey, Wales and the Midlands of England.

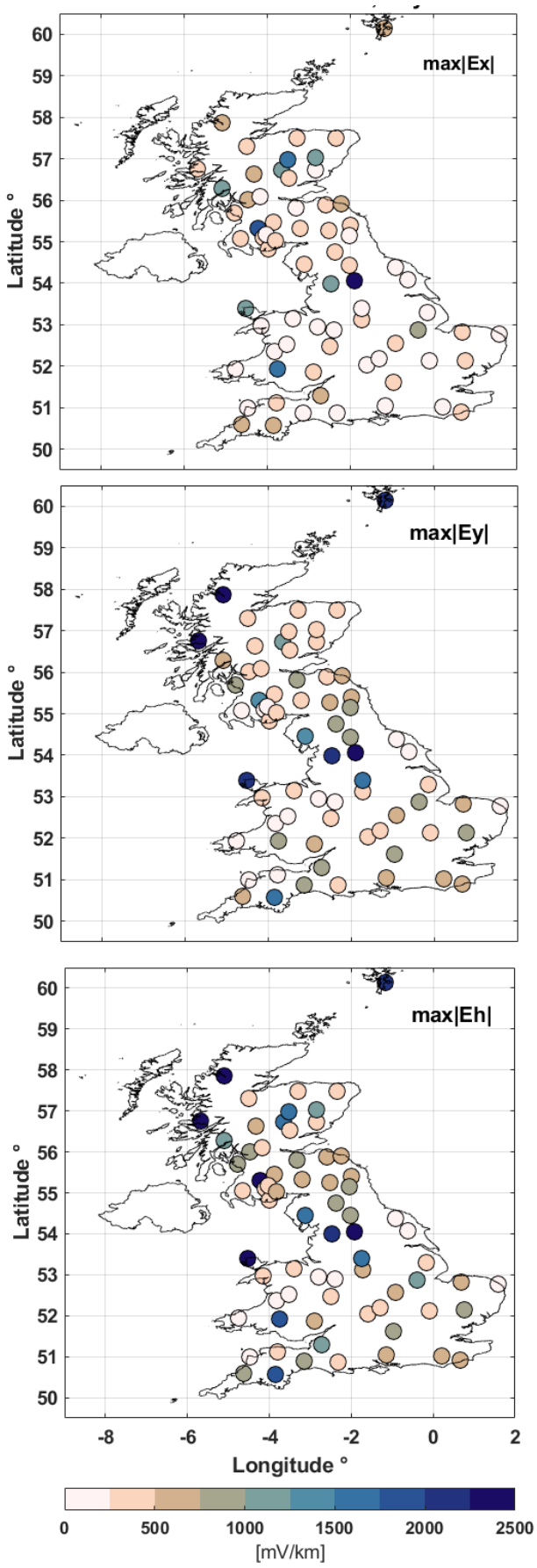

Figure 13: Maximum electric field values at each MT site during the September 2017 storm in the north (Ex), east (Ey) and total horizontal field (Eh). Units of milliVolts per km. The highest values of >2,000 mV/km were modelled for west of Scotland and Anglesey, Wales.

4.2 APPLICATION TO REAL-TIME NOW AND FORECASTING

The SAGE N4 project developed specific code for nowcasting and forecasting geoelectric field values from real time data measured at the UK observatories and from forecasts of the magnetic field in the UK created using L1 solar wind satellite data streams. The geoelectric field computation uses a BGS-developed thin-sheet model of conductivity and was written in Fortan90 code. As the SAGE now- and forecasting code is highly modularised, it is possible to replace the geoelectric field code within the Docker-Compose setup on the cloud service infrastructure that it presently in use (Amazon Web Services, AWS).

Figure 14 shows the workflow for the space weather ground impact prediction platform. It includes inputs of data and models to derive the GIC impact nowcast and forecast from SAGE and the outputs to the Met Office. The box labelled “Thin-sheet model” (central column) will be replaced by the updated “SAGE_MT_map” module. The new module consists of the MT impedance data and uses forward modelling of the magnetic field variation to compute the geoelectric field at each site and then interpolation to produce a 10 x 10 km grid cell map of the geoelectric field for the GIC computation modules. The code is written and evaluated in Python allowing easier future maintenance.

Beyond the end of the SAGE project, we envisage the use of the full 3D model of the UK conductivity. A 3D model can be used to predict the ground electric field during space weather events in real-time, for example using the approach developed by Kruglyakov *et al.*, (2022).

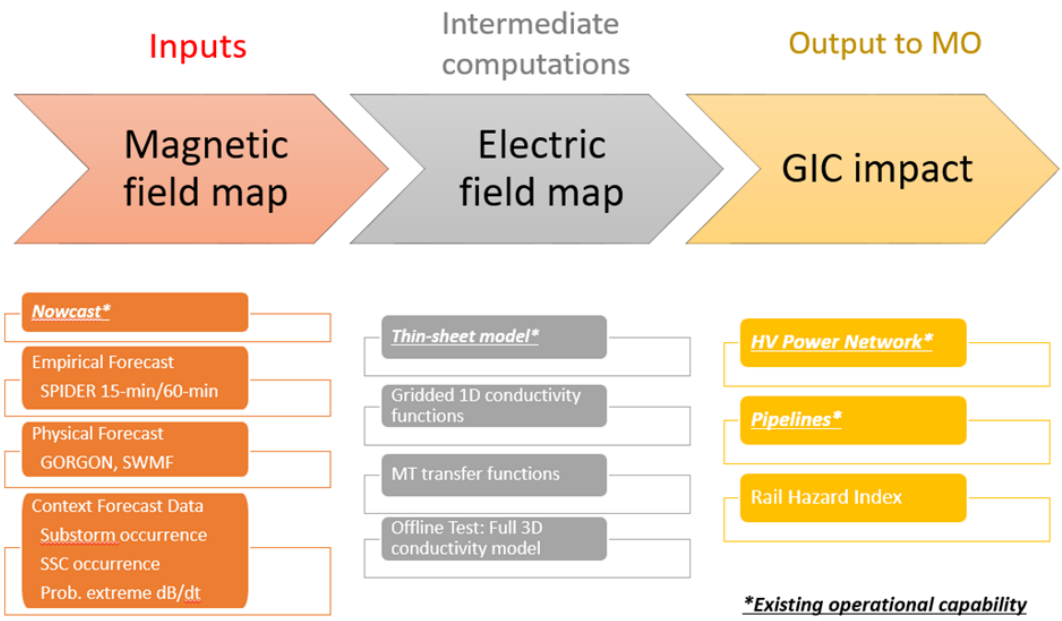

Figure 14: Workflow for SAGE ground impact modelling: inputs, processing and outputs.

4.2.1 Nowcasting methodology

For the nowcasting of geoelectric field maps using real-time magnetic data, we follow the approach developed by Malone-Leigh *et al.* (2023). The magnetic field measurements at the three UK geomagnetic observatories, provided at minute cadence, are interpolated across the UK. A timeseries of magnetic field variations in the Bx (north-south) and By (east-west) directions at all 70 MT sites are extracted for the past two days. The end of the timeseries is padded with a taper to zero for further 105 minutes into the future to reduce the end-effects from the FFT. This edge effect results in an under-estimation of electric fields at the end of the timeseries. A small scaling factor, adapted from Malone-Leigh *et al.,* is applied to account for the under-estimate.

Within the nowcasting code, the geoelectric field maps are updated every 5 minutes. The following steps are taken:

1. Magnetic field values for the previous two days to within the last five minutes (i.e. 1440x2=2880 points) from the three UK observatories are interpolated over modelling domain (using latitude weighting between the observatories).
2. Timeseries of Bx and By values from the interpolated magnetic field are extracted at each of the 70 MT locations.
3. The magnetic field timeseries is padded 105 minutes into the future following 'end-to-zero' approach (i.e. the last value in the timeseries is linearly interpolated to zero).
4. An FFT of the magnetic field variations at each MT location is computed and multiplied with impedance tensor. Then the inverse FFT is applied to derive timeseries of geoelectric field values in north-south and east-west direction (Ex and Ey).
5. Correction factors as outlined in Malone-Leigh *et al.* (2023) are applied to last 105 minutes of electric field data.
6. The peak value of geoelectric field in the whole modelling domain is estimated in the last five minutes of measurement time.
7. The peak values of the electric field are interpolated onto 10 x 10km grid across UK.
8. Finally, the largest peak values within the final timesteps for 'SAGE MT map' are found and used as input for GIC modelling code.

We slightly adapt the procedure from Malone-Leigh *et al.* (2023) of applying a correction factor to the last 105 data points in the forecast to compensate the edge effect at the end of the time series used in the FFT. In agreement, we found that the nowcast model underestimates the amplitude of the electric field when comparing it to the 'full model' (running the FFT on a full 2 day time window encompassing the full storm). Additionally, the MT derived geoelectric fields are often slightly smaller than the full measured field as discussed in Beggan *et al.* (2021). The correction factors in Malone-Leigh *et al.* (2023) were found to somewhat overestimate the electric fields specially at the peak times. This might be caused by regional differences in the geoelectric field between Ireland and Britain or by the authors' approach of using impedance tensors that are corrected for galvanic distortion, which is not the case in SAGE. We therefore use the adjusted nowcast correction curve for times t = [105, 1] minutes before now by factor *f*:

$$f(t) = \{-(3.0\ x\ 10^{-6}t^3) + (5.3\ x\ 10^{-4}t^2) - (3.0\ x\ 10^{-2}t) + 1.3\}\ .$$

An example using this methodology can be seen in Figure 15. We used the magnetic field data from Eskdalemuir observatory measured on 6-8 September 2017 and the local MT impedance to derive a nowcast of the geoelectric field. The corrected nowcast model captures the variations and amplitude of the geoelectric field very well. At ESK, geoelectric field data were collected during this period, providing the validation of this approach.

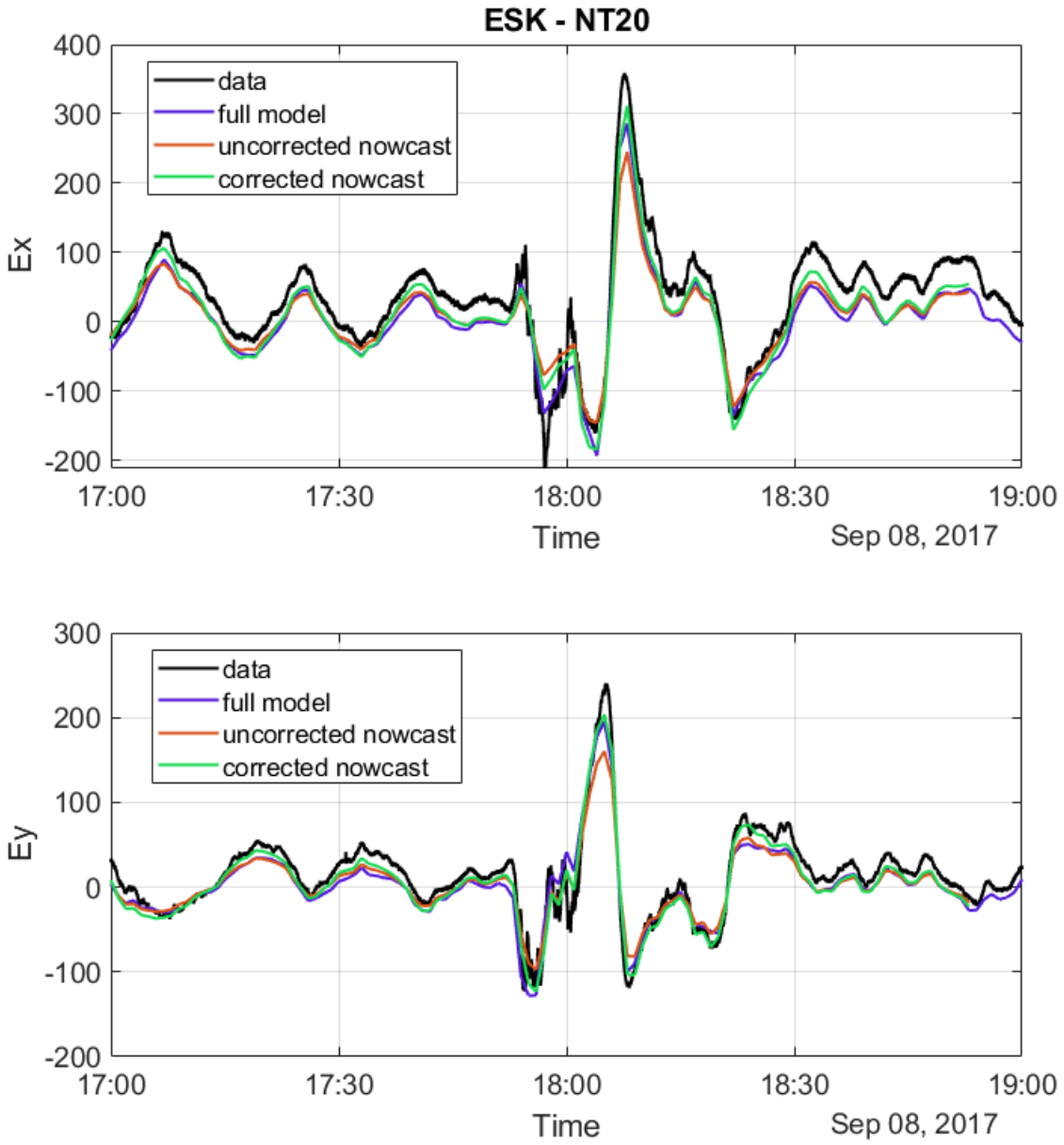

Figure 15: Electric field data and model at ESK observatory for the September 2017 storm. Comparison of measured data (black), modelled data (full model – purple, nowcast – red, corrected nowcast - green) illustrating the edge effect observed in the nowcast and the application of a correction factor to account for this.

4.2.2 Forecasting using Gorgon and Spider models

One limitation of the MT impedance FFT approach is that it requires continuous timeseries of the magnetic field at the ground to work correctly. This is generally guaranteed when using the UK observatory data, given they have excellent redundancy and are maintained specifically for real-time operations.

In the forecasting modules of SAGE, however, the predicted magnetic field from the physics-based and machine learning models does not necessarily provide continuous magnetic field data. In particular, this relates to the 'gappy' delivery of data from the DSCOVR and ACE satellites and the general lack of continuous data (Smith *et al.*, 2022).

Gorgon predicts the magnetic field from the L1 point data, with the predicted data starting at 30 minutes in the future after it is triggered. It will be necessary to pad the data gaps to use the frequency-domain approach that requires continuous timeseries of the magnetic field.

4.3 EXTREME VALUE ANALYSIS OF MT-DERIVED GEOELECTRIC FIELDS

With the new MT dataset, it is now possible to perform extreme value analysis (EVA) to explore probabilities or return values for large geoelectric field values across the UK. While a full analysis is beyond the scope of this project, we illustrate how the new data set can inform existing knowledge of the potential for extreme geoelectric fields.

We computed geoelectric fields for 44 years of geomagnetic data (1980-2023) at the MT site locations, using the magnetic field data sampled at 1-min from the closest UK observatory (ESK, HAD). For a more complete study, the magnetic field at each location should be derived from interpolation of all available magnetic field data.

We then performed extreme value analysis to estimate 40- and 100-year return levels with the open-source python package *pyextremes*[5] using 12h windows to exclude correlated events. Other methods will be explored in a more detailed analysis.

Figure 16 shows the estimated values and range from a 1-in-100 year return period using the 99.97th percentile of the modelled geoelectric field values over the 44 years of magnetic data available. The left panel shows the expected values at the three geomagnetic observatories. The right panel shows the extreme values for five MT sites (see Table 1 for locations). A value of 10,000 mV/km is equal to 10 V/km which would be an extreme value to experience in Britain.

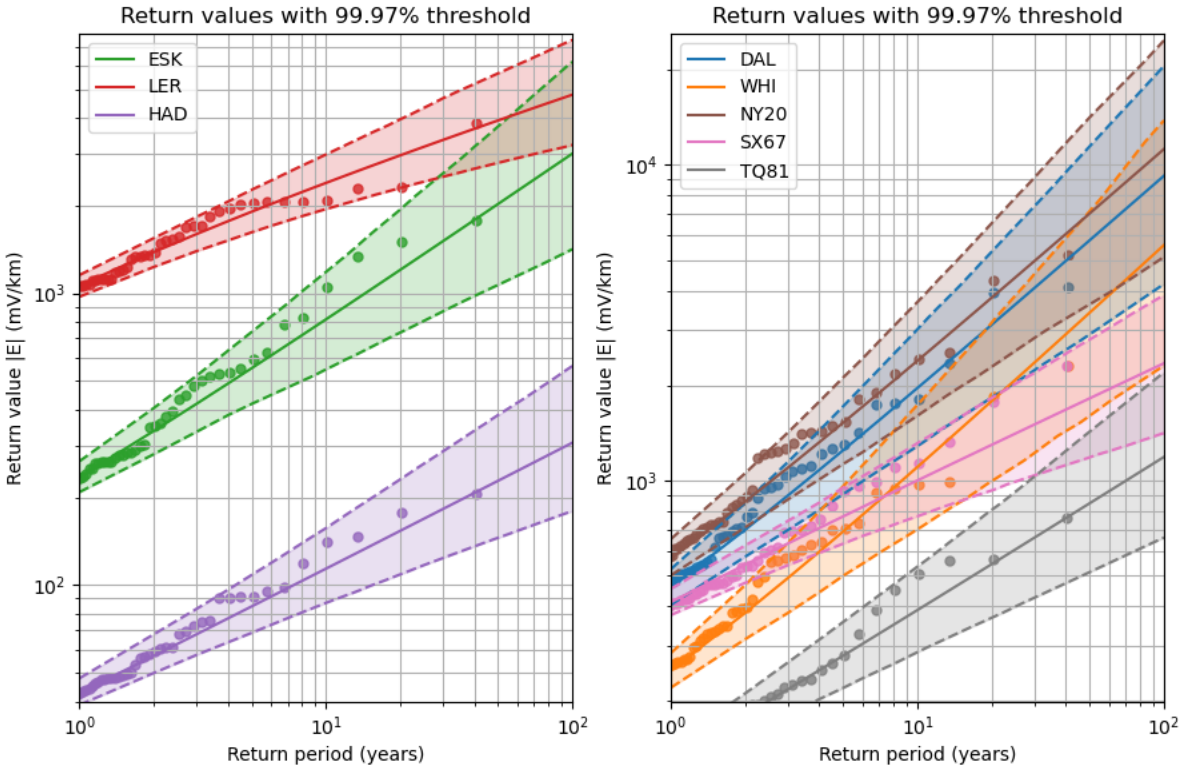

Figure 16: The 100-year return values for horizontal electric field magnitude (|E|) at UK observatories (left) and selected MT sites (right) using a 99.97% threshold, presented in Huebert *et al.* (2023).

[5] https://georgebv.github.io/pyextremes/

5 Summary and future work

The results presented in the previous section are the first steps towards a more thorough model of local inhomogeneities in the electric field and from these we can analyse how much they influence the GIC estimates.

With the SAGE MT data collection completed, a PhD project at the University of Edinburgh has been focussing on inverse modelling of the new MT data set using state-of-the-art parallelised computer algorithms, such as ModEM (Kelbert *et al.,* 2014), which can fully discretise the model space in three dimensions and include onshore topography and offshore bathymetry. Bathymetry is particularly important because the electric currents that flow in salty sea water affect the data at significant distances from the coast. New efforts have been made to better characterize offshore near-coastal sediments and their conductance (*Grayver*, 2021).

With the new 3D model of electrical conductivity, it will be possible to predict the geoelectric field on a regular grid across the British Isles, taking into account prior information like bathymetry and off-shore sediment thickness. This model will also allow a more physical interpolation of the geoelectric field between MT site locations because the electrical conductivity in model cells between MT sites.

In this report we provide a description of an extensive effort to collect high quality magnetotelluric data across mainland Britain between 2021 and 2024. The MT data show the large variability of the geologically diverse island and the localised nature of the geoelectric field and its effect on space weather impacts.

Appendix 1

The appendix contains a table with station locations for reference. The following abbreviations are used: BGS – British Geological Survey; UoE – University of Edinburgh; UoS – University of Southampton; for other references see text. Figure 17 to Figure 22 provide a visualisation of the magnetotelluric transfer (impedance) functions at sixty MT sites in the UK.

Table 1: Complete list of MT site locations and coordinates of deployment.

#	Grid ref	Location	Latitude	Longitude	Collected by
1	NY90	Richmond	54.44067	-2.026022	BGS
2	NY20	Lakes	54.44425	-3.1134318	BGS
3	SE06	Appletreewick	54.04938	-1.9106625	BGS
4	SD65	Forest of Bowland	53.986667	-2.465556	BGS
5	SE69	North Yorkshire moors	54.3846	-0.9251643	BGS
6	SE86	Scarborough	54.07972	-0.6292771	BGS
7	SK15	Derbyshire	53.11447	-1.7259096	BGS
8	SJ73	Market Drayton	52.88483	-2.4068719	BGS
9	SJ43	Wrexham	52.93861	-2.8035257	BGS
10	SJ06	Denbigh	53.13584	-3.3985801	BGS
11	TF28	Lincoln	53.30499	-0.1553931	BGS
12	SO68	Shropshire Hills	52.46889	-2.4906282	BGS
13	SH39	Anglesey	53.39774	-4.5262569	BGS
14	TF03	Grantham	52.86825	-0.3847609	BGS
15	SN99	Caersws	52.52497	-3.532127	BGS
16	SH54	Porthmadog	52.97288	-4.1587406	BGS
17	NY73	Alston	54.74057	-2.375525	BGS
18	NT91	Alnham	55.40232	-2.0077226	BGS
19	NY69	Kielder Forest	55.25962	-2.5340485	BGS
20	NX75	Dumfries	54.83088	-3.9921238	BGS
21	NY98	Kirkwhelpington	55.15623	-2.0391719	BGS
22	NT15	Nine Mile Burn	55.81058	-3.3223916	BGS
23	SP79	Market Harborough	52.56506	-0.9225294	BGS
24	TL34	Cambridge	52.1239	-0.1012329	BGS
25	TF82	Houghton Hall	52.82396	0.69672383	BGS
26	TL85	Shimpling	52.14081	0.75420	BGS
27	SU52	Hinton Ampner	51.03599	-1.1563144	BGS
28	SP45	Banbury	52.1887	-1.3062458	BGS
29	TG42	Long Gores Marsh	52.76779	1.5909811	BGS
30	TQ81	Pett Level	50.9034056	0.6719138	BGS
31	SK18	Ladybower	53.3895324	-1.7374847	BGS
32	SU79	Christmas Common	51.6164452	-0.9716366	BGS
33	SX17	Bodmin Moor	50.5879194	-4.6231356	BGS
34	SX67	Dartmoor	50.5759945	-3.8506735	BGS
35	SS73	Exmoor	51.114178	-3.795733	BGS

36	ST10	Blackdown Hills	50.8784496	-3.1471857	BGS
37	ST70	Hazelbury Bryan	50.8768435	-2.320163	BGS
38	ST45	Cheddar Gorge	51.2888077	-2.7318644	BGS
39	SO31	East Brecon Beacons	51.8629119	-2.8898606	BGS
40	SN72	West Brecon Beacons	51.9252425	-3.7557944	BGS
41	SN12	Pembrokeshire	51.9327885	-4.7636344	BGS
42	SN77	Aberystwyth University	52.36339	-3.827999	BGS
43	SP23	Burmington	52.0377501	-1.6052112	BGS
44	TQ52	High Weald AONB	51.0269178	0.2157529	BGS
45	NS64	Kippen	56.0948604	-4.1764613	UoE+BGS
46	NH42	Drumnadrochit	57.30094	-4.49182	UoE+BGS
47	NH19	Leckmelm	57.8625709	-5.0935414	UoE+BGS
48	NM76	Acharacle	56.75419169	-5.68861236	UoE+BGS
49	NN01	Inveraray	56.28727531	-5.106662385	UoE+BGS
50	NS81	Abington	55.4574381	-3.8635646	UoE+BGS
51	NJ74	Turriff	57.491355145	-2.35531994	UoE+BGS
52	NX37	Newton Stewart	55.06195872	-4.656046205	UoE+BGS
53	NO46	Forfar	56.72884	-2.85449067	UoE+BGS
	Observatories:				
54	HU43	Lerwick observatory	60.13785	-1.18217	BGS
55	NT20	Eskdalemuir observatory	55.314	-3.206	BGS
56	SS22	Hartland observatory	50.995	-4.483	BGS
	Legacy sites:				
57	NT66	Whiteadder	55.88319	-2.590969	BGS (SWIGS)
58	NS24	Dalry	55.70406	-4.788223	BGS (SWIGS)
59	NS48	CAL	56.00383	-4.47333548	UoS (SWIGS)
60	NJ24	ELC	57.48527	-3.29782519	UoS (SWIGS)
61	NO08	MAR	56.97714	-3.51986602	UoS (SWIGS)
62	NN55	RAN	56.64078	-4.329662	UoS (SWIGS)
63	NO49	TAN	57.0344	-2.853744	UoS (SWIGS)
64	NO03	Birnam Wood (Birn)	56.52331	-3.49723	Junge *et al.*
65	NT86	Laveric Law	55.90761	-2.23836	Junge *et al.*
66	NN96	Pitlochry (Pilo)	56.72433	-3.66048	Junge *et al.*
67	NX87	Barfil	55.03643	-3.817304	Tauber *et al.*
68	NS50	Carsphairn Forest	55.31079	-4.217883	Tauber *et al.*
69	NX68	Holy Linn Waterfall	55.10922	-4.105575	Tauber *et al.*
70	NX78	Minnygryle Hill	55.18504	-4.031792	Tauber *et al.*

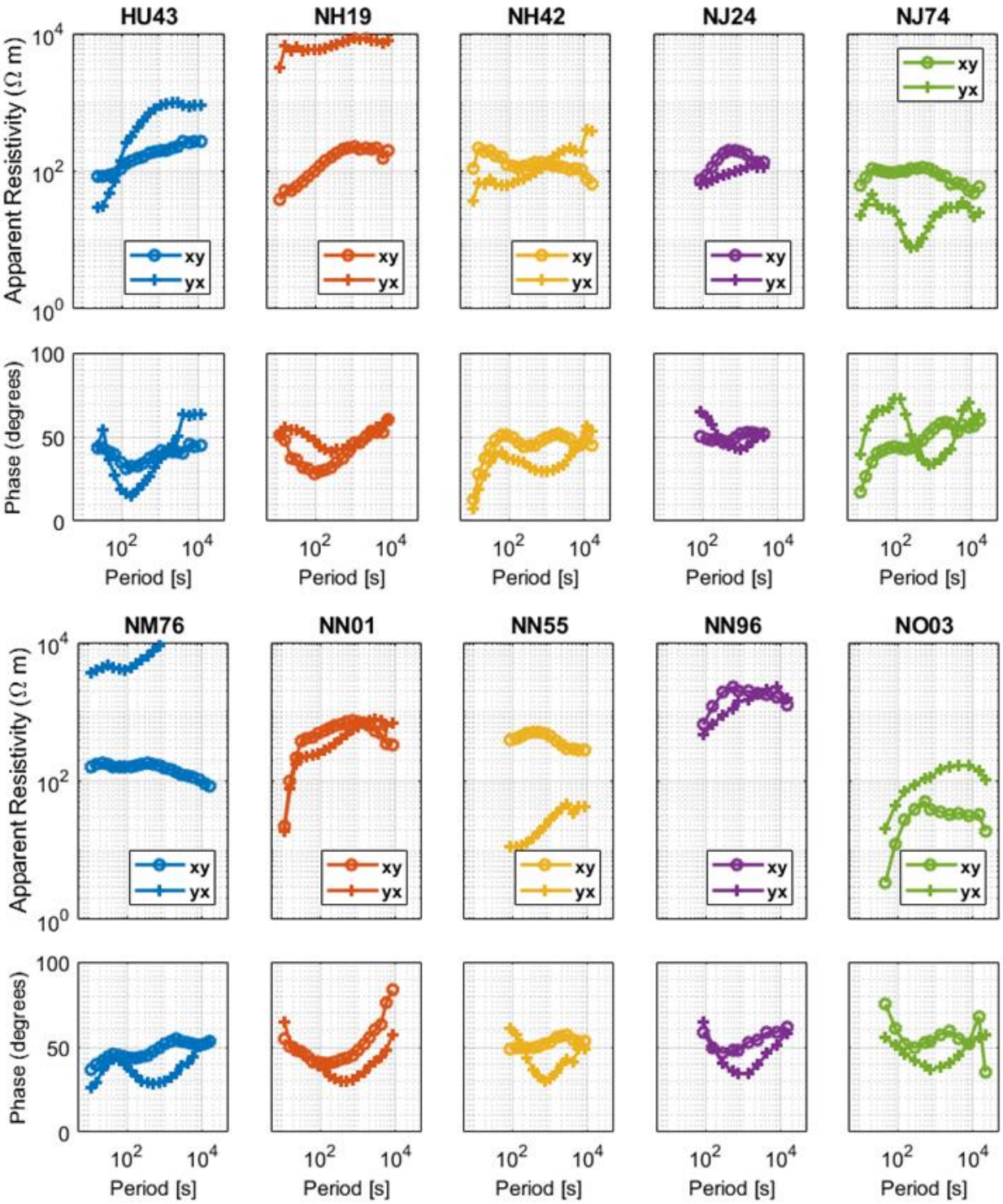

Figure 17: Apparent resistivity (upper) and phase (lower panels) of the main components Zxy and Zyx of the MT impedance tensor at 10 locations in the UK.

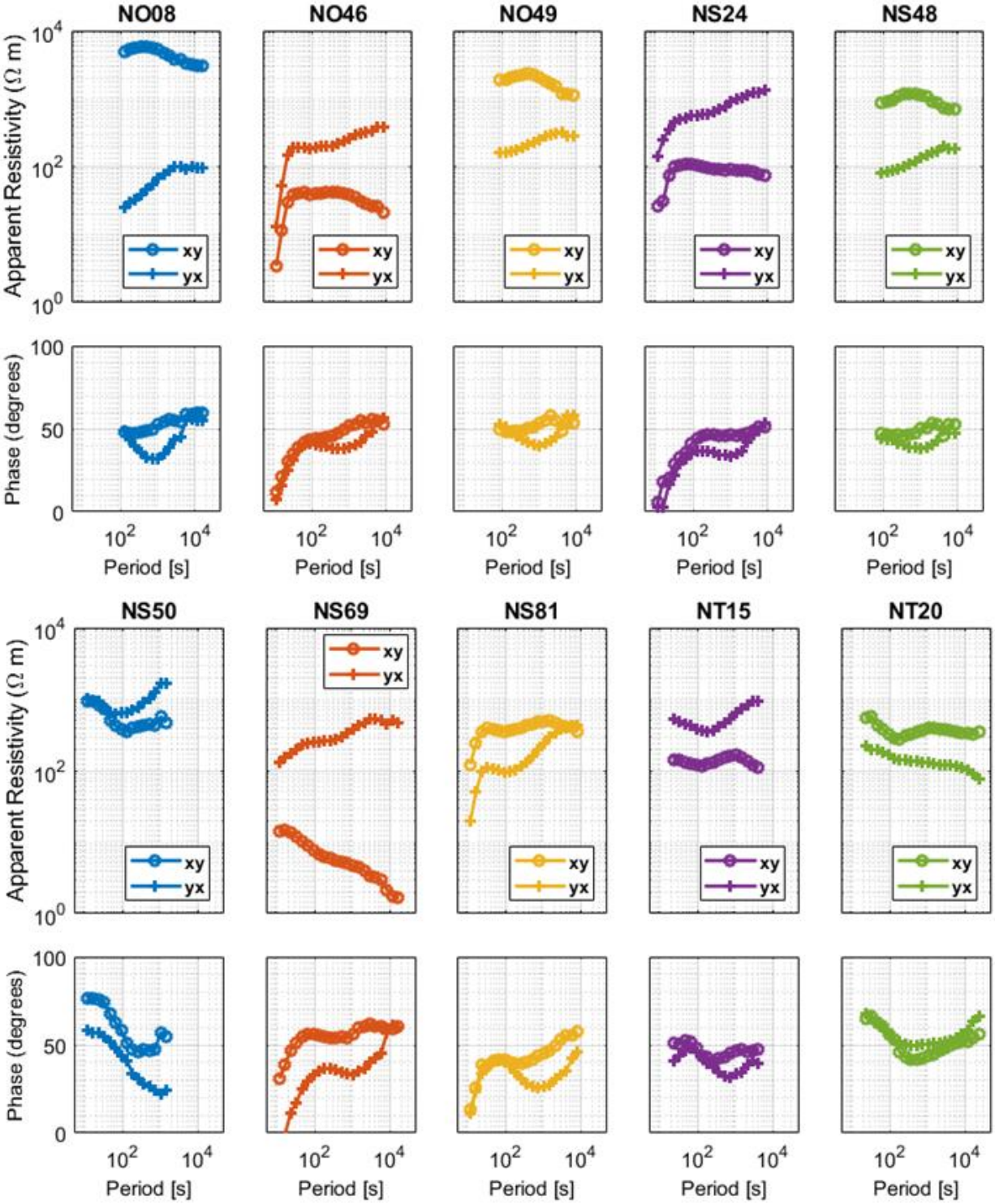

Figure 18: Apparent resistivity (upper) and phase (lower panels) of the main components Zxy and Zyx of the MT impedance tensor at 10 locations in the UK.

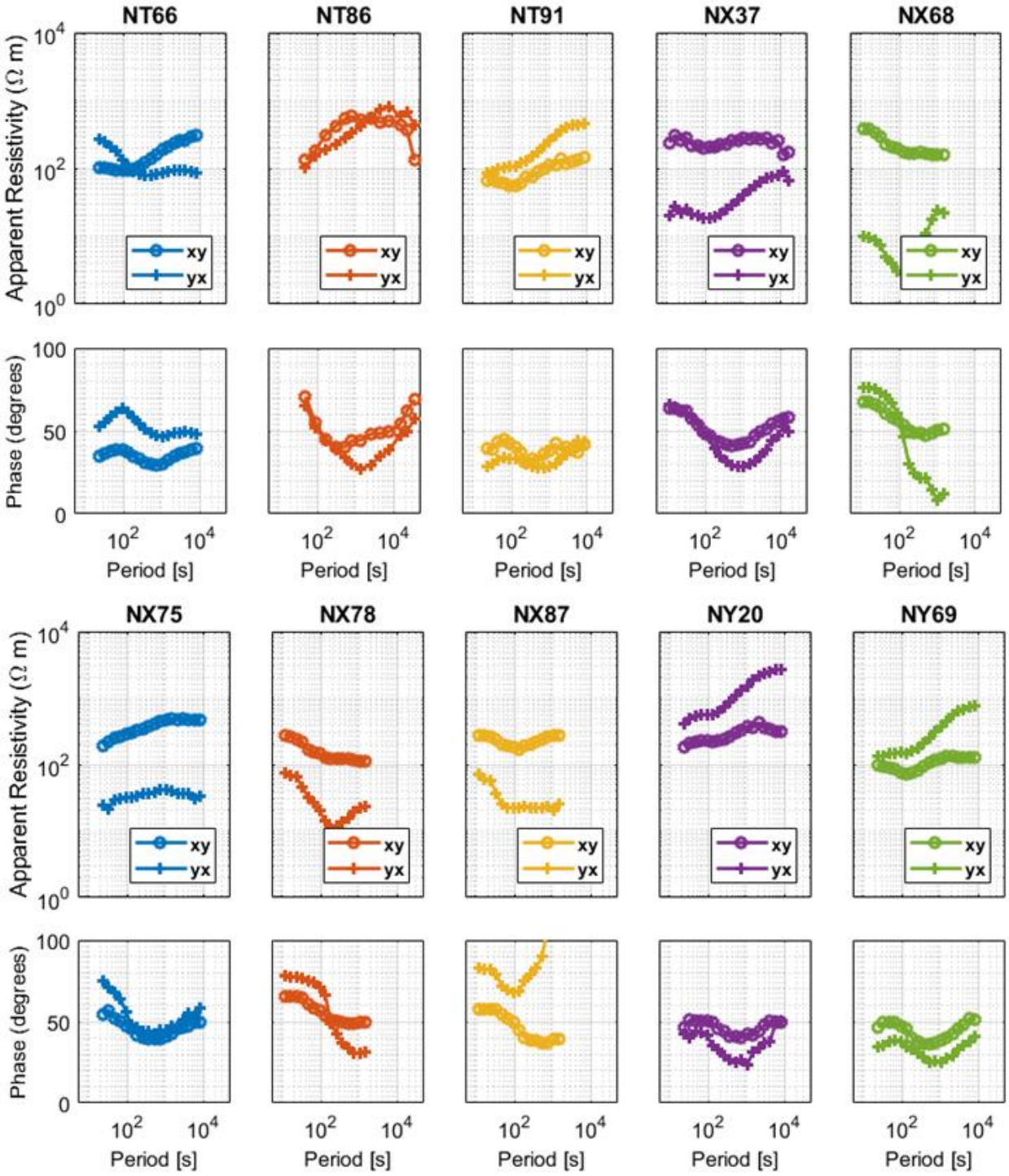

Figure 19: Apparent resistivity (upper) and phase (lower panels) of the main components Zxy and Zyx of the MT impedance tensor at 10 locations in the UK.

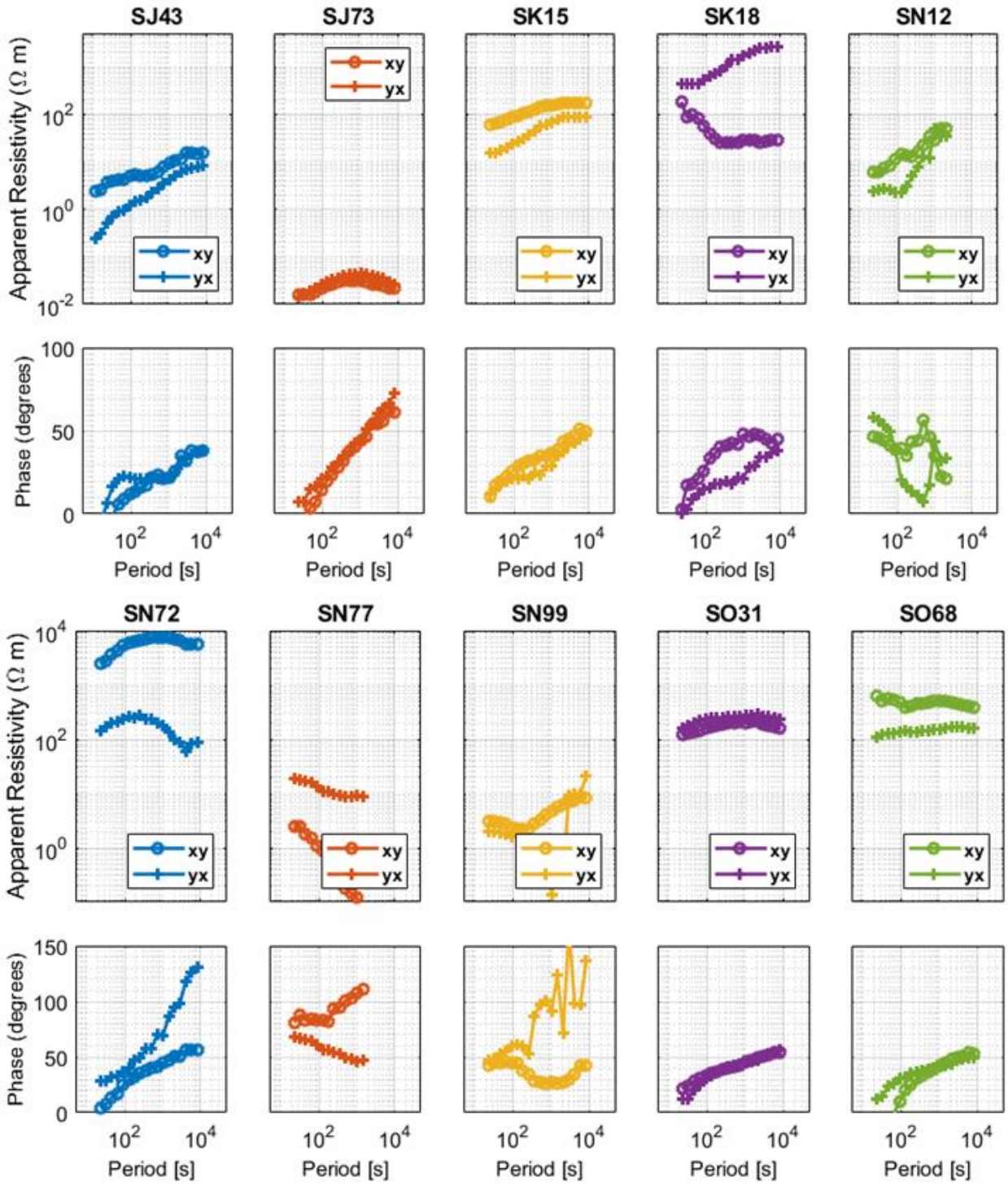

Figure 20: Apparent resistivity (upper) and phase (lower panels) of the main components Zxy and Zyx of the MT impedance tensor at 10 locations in the UK.

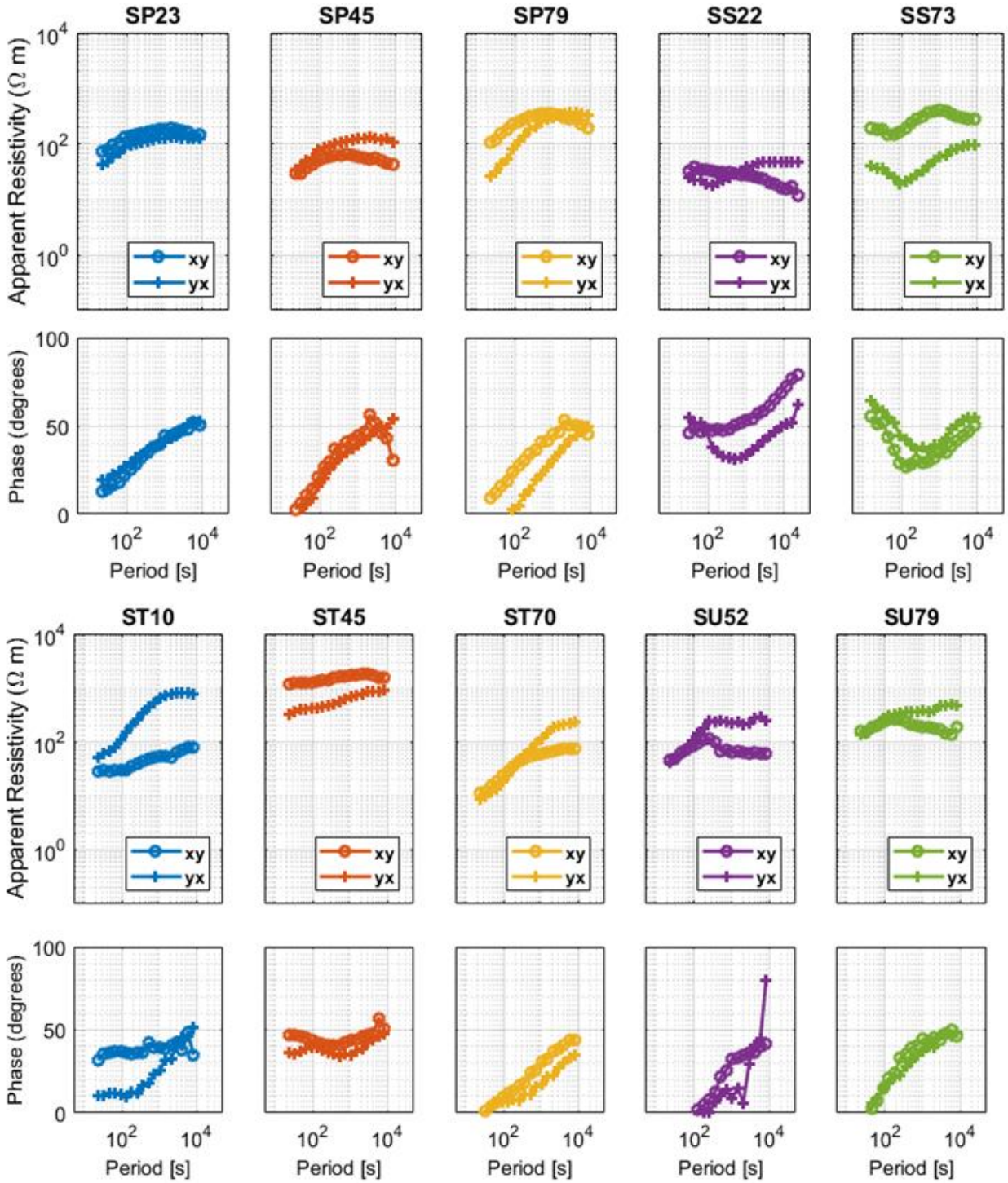

Figure 21: Apparent resistivity (upper) and phase (lower panels) of the main components Zxy and Zyx of the MT impedance tensor at 10 locations in the UK.

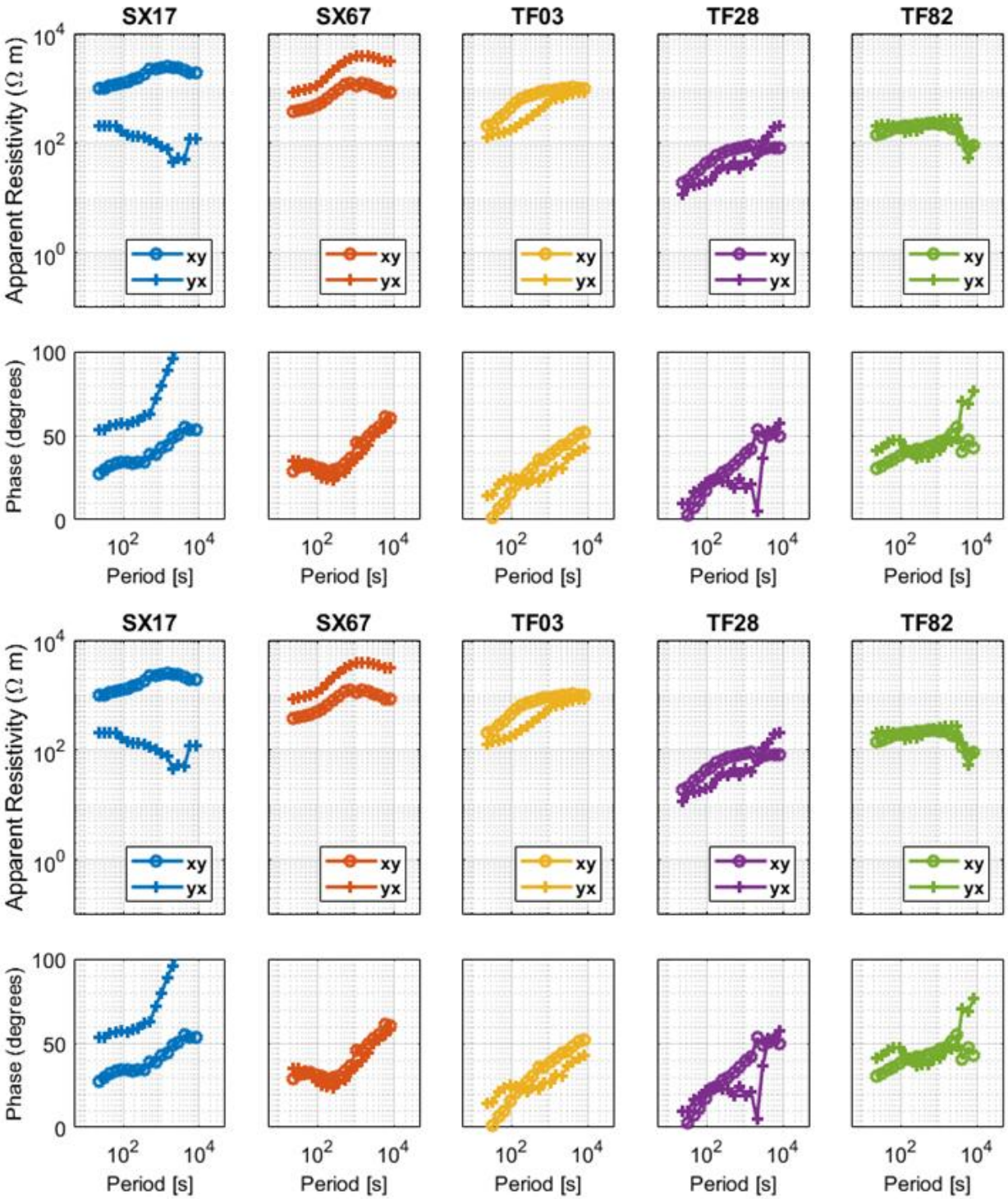

Figure 22: Apparent resistivity (upper) and phase (lower panels) of the main components Zxy and Zyx of the MT impedance tensor at 10 locations in the UK.

Glossary

EM induction - Electromagnetic induction, describing the connected effects and interaction of time-varying electric and magnetic fields.

GIC – Geomagnetically induced currents (GICs) are generated from strong ground electric fields during geomagnetic storms.

Ground electric or geoelectric field (GEF) is induced by variations in the magnetic field over a wide frequency/period range. Can be measured with electric dipoles.

Magnetotelluric (MT) method - passive geophysical deep-sounding techniques. MT uses simultaneous measurements of the natural variations in the electric and magnetic field at the Earth's surface to image the conductivity distribution in the subsurface.

Long-period MT – typically, signal periods >10s are investigated using fluxgate magnetometers

Broadband MT – including higher frequency data, typically 1000Hz – 10s

Magnetotelluric (MT) impedance tensor – transfer function between horizontal magnetic and electric field changes under a plane-wave assumption. The tensor is frequency dependent and complex.

SWIMMR-SAGE Space Weather Instrumentation, Measurement, Modelling and Risk– Activities in Ground Effects, NERC-STFC programme.

References

AYALA, C., ET AL. (2022), Geomagnetism, Paleomagnetism and Electromagnetism Perspectives on Integrated, Coordinated, Open, Networked (ICON) Science, *Earth and Space Science*, 9(6), e2021EA002141.

AMM, O. (1997), Ionospheric elementary current systems in spherical coordinates and their application, Journal of Geomagnetism and Geoelectricity, Volume 49 (7), page 947-955, 10.5636/jgg.49.947.

BAILLIE, O.. (2020), The Investigating geoelectric tides at three geomagnetic observatories in the UK,.MSCR THESIS, THE UNIVERSITY OF EDINBURGH

BEAMISH, D. (2012), The 1:625k near-surface bedrock electrical conductivity map of the UK, BGS REPORT.

BEAMISH, D., (2013). The bedrock electrical conductivity map of the UK. *Journal of Applied Geophysics*, 96, 87–97. 10.1016/j.jappgeo.2013.06.001

BEGGAN, C.D., (2015) Sensitivity of geomagnetically induced currents to varying auroral electrojet and conductivity models, *Earth, Planets and Space*, 67 (1), 1-12, 10.1186/s40623-014-0168-9

BEGGAN, C. D., G. S. RICHARDSON, O. BAILLIE, J. HÜBERT, AND A. W. P. THOMSON (2021), Geoelectric field measurement, modelling and validation during geomagnetic storms in the UK, *Journal of Space Weather and Space Climate*, 11.

BEGGAN, C. D. AND MARPLE, S. R.: BUILDING A RASPBERRY PI SCHOOL MAGNETOMETER NETWORK IN THE UK, GEOSCI. COMMUN., 1, 25–34, HTTPS://DOI.ORG/10.5194/GC-1-25-2018, 2018.

BOLDUC, L., (2002) GIC observations and studies in the Hydro-Québec power system. *J Atmos Sol-Terr Phy.,* 64. 10.1016/S1364-6826(02)00128-1.

BOTELER, D. H., (2006) The super storms of August/September 1859 and their effects on the telegraph system., *Advances in Space Research*, 38(2), 159 – 172. 10.1016/j.asr.2006.01.013

BOTELER, D. H., 2019. A 21st Century View of the March 1989 Magnetic Storm. *Space Weather*, 17, 1–15 10.1029/2019SW002278.

CALDWELL, T.G., H.M. BIBBY, and C. BROWN, The magnetotelluric phase tensor, *Geophysical Journal International*, Volume 158, Issue 2, August 2004, Pages 457–469, https://doi.org/10.1111/j.1365-246X.2004.02281.x

CAMPANYA, J., P. T. GALLAGHER, S. P. BLAKE, M. GIBBS, D. JACKSON, C. D. BEGGAN, G. S. RICHARDSON, AND C. HOGG (2019), Modeling Geoelectric Fields in Ireland and the UK for Space Weather Applications, *Space Weather*, 17(2), 216-237.

EGBERT, G. D. (1997), Robust multiple-station magnetotelluric data processing, *Geophysical Journal International*, 130(2), 475–496-475–496.

GAMBLE, T.D., GOUBAU, W. M.AND J. CLARKE, (1979), "MAGNETOTELLURICS WITH A REMOTE MAGNETIC REFERENCE," *GEOPHYSICS* 44: 53-68.GRAYVER, A. V. (2021), Global 3-D Electrical Conductivity Model of the World Ocean and Marine Sediments, *Geochemistry, Geophysics, Geosystems*, 22(9), e2021GC009950.

HÜBERT, J., C. D. BEGGAN, G. S. RICHARDSON, T. MARTYN, AND A. W. P. THOMSON (2020), Differential Magnetometer Measurements of Geomagnetically Induced Currents in a Complex High Voltage Network, *Space Weather*, 18(4), e2019SW002421.

HÜBERT, J., ORR, L., BEGGAN, C., EATON, E., RICHARDSON, G. (2023): EXTREME VALUES AND RETURN LEVELS OF MODELLED GEOELECTRIC FIELDS FOR THE UNITED KINGDOM USING NEW MAGNETOTELLURIC DATA, XXVIII GENERAL ASSEMBLY OF THE INTERNATIONAL UNION OF GEODESY AND GEOPHYSICS (IUGG) (BERLIN 2023). HTTPS://DOI.ORG/10.57757/IUGG23-2581

HÜBERT, J., C. D. BEGGAN, G. S. RICHARDSON, N GOMEZ-PEREZ, A. COLLINS AND A.W.P. THOMSON (2024), Validating a UK geomagnetically induced current model using differential magnetometer measurements, *Space Weather*, 22(2), e2023SW003769.

KELBERT, A. (2020), The Role of Global/Regional Earth Conductivity Models in Natural Geomagnetic Hazard Mitigation, *Surveys in Geophysics*, 41(1), 115-166.

JANKOWSKI, J. SUCKSDORFF, C. (1996), The IAGA guide for magnetic measurements and observatory practice, *International Association of Geomagnetism and Aeronomy*

KELBERT, A., N. MEQBEL, G. D. EGBERT, AND K. TANDON (2014), ModEM: A modular system for inversion of electromagnetic geophysical data, *COMPUTERS & GEOSCIENCES*, 66, 40-53.

KRUGLYAKOV, M., A. KUVSHINOV, AND E. MARSHALKO (2022), Real-Time 3-D Modeling of the Ground Electric Field Due To Space Weather Events. A Concept and Its Validation, *Space Weather*, 20(4).

LOVE, J. J., G. M. LUCAS, A. KELBERT, and P. A. BEDROSIAN, (2018) Geoelectric Hazard Maps for the Mid-Atlantic United States: 100 Year Extreme Values and the 1989 Magnetic Storm. *Geophysical Research Letters*, 45(1), 5–14. 10.1002/2017GL076042

LUCAS, G. M., J. J. LOVE, AND A. KELBERT (2018), Calculation of Voltages in Electric Power Transmission Lines During Historic Geomagnetic Storms: An Investigation Using Realistic Earth Impedances, *Space Weather*, 16(2), 185-195.

MCKAY, A. (2003), Geoelectric fields and Geomagnetically Induced Currents in the United Kingdom. Ph.D. thesis, University of Edinburgh. http://hdl.handle.net/1842/639.

MCLAY, S. A. and BEGGAN, C. D.: Interpolation of externally-caused magnetic fields over large sparse arrays using Spherical Elementary Current Systems, Ann. Geophys., 28, 1795–1805, https://doi.org/10.5194/angeo-28-1795-2010, 2010.

MURPHY, B. S., G. M. LUCAS, J. J. LOVE, A. KELBERT, P. A. BEDROSIAN, AND E. J. RIGLER (2021), Magnetotelluric Sampling and Geoelectric Hazard Estimation: Are National-Scale Surveys Sufficient?, *Space Weather*, 19(7).

OUGHTON, E. J., M. HAPGOOD, G. S. RICHARDSON, C. D. BEGGAN, A. W. P. THOMSON, ET AL. (2018), A Risk Assessment Framework for the Socioeconomic Impacts of Electricity Transmission Infrastructure Failure Due to Space Weather: An Application to the United Kingdom. *Risk Analysis*, 38(12), 1–22 10.1111/risa.13229

PULKKINEN, A., E. BERNABEU, J. EICHNER, C. BEGGAN, and A. THOMSON (2012), Generation of 100-year geomagnetically induced current scenarios. *Space Weathe*r, 10, S04,003. 10.1029/2011SW000750.

ROGERS, N. C., J. A. WILD, E. F. EASTOE, J. W. GJERLOEV, and A. W. P. THOMSON (2020), A global climatological model of extreme geomagnetic field fluctuations. *J. Space Weather Space Clim*., 10, 5, 10.1051/swsc/2020008

ROSENQVIST, L., T. FRISTEDT, A. P. DIMMOCK, P. DAVIDSSON, R. FRIDSTRÖM, ET AL. (2022), 3D Modeling of Geomagnetically Induced Currents in Sweden — Validation and Extreme Event Analysis. *Space Weather*,20(3), e2021SW002,988. 10.1029/2021SW002988.

SIMPSON, F., and K. BAHR (2021), Nowcasting and validating Earth's electric-field response to extreme space-weather events using magnetotelluric data: application to the September 2017 geomagnetic storm and comparison to observed and modelled fields in Scotland. *Space Weather*, 19, e2019SW002,432, 10.1029/2019SW002432

SMITH, A. W., FORSYTH, C., RAE, I. J., GARTON, T. M., JACKMANN, C. M., BAKRANIA, M., et al. (2022). On the considerations of using near real time data for space weather hazard forecasting. *Space Weather*, 20, e2022SW003098. https://doi.org/10.1029/2022SW003098

SMIRNOV, M. (2008), Magnetotelluric data processing with a robust statistical procedure having a high breakdown point. *Geophysical Journal International*, 152(1), 1–7. 10.1046/j.1365-246X.2003.01733.x.

TAUBER, S., R. BANKS, O. RITTER, U. WECKMANN, AND A. JUNGE (2003), A high-resolution magnetotelluric survey of the Iapetus Suture Zone in southwest Scotland, *Geophysical Journal International,* 153(3), 548-568.

THOMSON, A. W. P., E. DAWSON, and S. REAY (2011), Geomagnetic Extreme Statistics for Europe. *Space Weather*, 9, S10,001. 10.1029/2011SW000696

VASSEUR, G., AND P. WEIDELT (1977), Bimodal electromagnetic induction in non-uniform thin sheets with an application to the northern Pyrenean induction anomaly, *Geophys. J. R. Astr*. SOC., 51, 669-690.